Inês Gonçalves Tavares

Bachelor of Science in Micro and Nanotechnologies Engineering

Triplet-to-Singlet energy transfer as a novel triplet harvesting mechanism: Photophysics and prototype OLED devices

Dissertation submitted in partial fulfilment
of the requirements for the degree of

Master of Science in
Micro and Nanotechnologies Engineering

Advisor:	Fernando Baião Dias, Associate Professor, Durham University
Co-Advisor:	Luís Miguel Nunes Pereira, Associate Professor, NOVA University of Lisbon

Chair	Prof. Dr Rodrigo Martins
Rapporteurs	Prof. Dr João Carlos Lima
Member	Prof. Dr Luís Pereira

October 2019

FACULDADE DE CIÊNCIAS E TECNOLOGIA
UNIVERSIDADE NOVA DE LISBOA

Triplet-to-Singlet energy transfer as a novel triplet harvesting mechanism: Photophysics and prototype OLED devices

“A diamond is a chunk of coal that
did well under pressure.”

- Henry Kissenger

Acknowledgements

Besides all the effort made during these months, all this work would never be possible without the guidance and support of some special persons whom I wish to sincerely thank.

To Science and Technology Faculty (FCT-UNL) for being my second home in these five years, for the excellence and the amazing campus.

To Materials Science Department (DCM) for the opportunity, quality teaching and excellent relation established between teachers, researchers and students.

To Prof Rodrigo Martins and Prof Elvira Fortunato for creating an academic path in Portugal highly focused on future technologies, providing all the facilities available for students' development and, for all the support and encouragement to follow with my project, NaNu.

The biggest thank you to my advisor Prof Fernando Dias for allowing me to work on the Organic Electroactive Materials (OEM) group and for giving me the opportunity and resources to work in this emergent area, as well as all the support, patience and guidance. I hope that the results obtained after these months meet his expectations.

To my co-advisor Prof Luis Pereira for his knowledge and passion for science, for always being ready to help me over these five years and for unknowingly arousing in me the interest in optoelectronics.

I am also grateful to everyone in the OEM group. Marc, Andrew, Patrycjia, Rongjuan, Larissa, Kleitos, Alastair, Chunyong, Yun and Erkan, as well as to Prof Andrew Monkman for the friendship, good vibes, fantastic collaboration and all the Friday beers. A special thanks to Piotr for his large expertise, patience and help during my stay in Durham. From our lessons of Lithuanian, I have something to say to the OEM group, AČIŪ!

Ao Daniel Pereira pela amizade, pelos bons momentos e por todos os conselhos. Obrigado por me teres feito sentir em casa num país que não era o meu.

To Asko Uri and Erki Enkvist from the University of Tartu, Estonia, for developing the ARC-1476 molecule that served as the study for this dissertation.

To the *13th International Conference on Optical Probes of Organic and Hybrid Optoelectronic Materials and Applications* organizers for allowing me to share my work at the conference and for the excellent experience.

To Durham University and its staff for warmly receive me and for supporting my participation in the *OP2019* conference.

Aos meus pais, Carlos e Helena. Devo-lhes tudo. Devo-lhes a pessoa que sou hoje, por todo o apoio incondicional, incentivo e presença em todas as etapas da minha vida. Pelo sacrifício feito para que eu pudesse sempre seguir os meus sonhos, o mais sincero obrigado!

Aos meus padrinhos, Sandra e Jaime, por moldarem a minha maneira de ver o mundo e por cultivarem a minha vontade de conhecer e saber.

Á minha família, pela união, pelos ensinamentos, pelo convívio, pelos típicos almoços de sábado que tanto senti falta durante estes meses de ausência e por sempre acreditarem em mim e naquilo que faço. Um agradecimento especial aos meus primos, Luís, Eduardo, Cláudio e Rodrigo, por todas as brincadeiras partilhadas, pelas conversas e por saber que tenho sempre com quem contar e quem me

proteja. Ao Cláudio e à Daniela agradeço o enorme voto de confiança por me escolherem como madrinha do Afonso, algo que me enche o coração de orgulho todos os dias.

Ao Bernardo, por todo o apoio, força, paciência e compreensão. Obrigado por acreditares que sou capaz, pelas palavras de coragem e por lutares a meu lado para atingirmos os nossos objetivos. Obrigado pelos sorrisos e pelo teu olhar.

Á Mafalda e ao João, por se terem tornado família. Obrigado por tudo!

Á malta do Success, ao Joan, ao Fred e ao Matos. Obrigado pelos momentos e conversas parvas, pelos convívios, idas ao fórum, viagens, pelas invasões à minha casa, e por sempre comerem o que eu cozinho, sem reclamar. Ao Opinião, pela sua constante animação e por ser a pessoa que tem sempre as palavras certas para me dizer. Ao Recife, por me mostrar que sou capaz de me superar a mim mesma, por todos os ensinamentos e pela amizade.

Aos afilhados que a faculdade me trouxe, a quem eu desejo todo o sucesso pessoal e profissional. Obrigado pela confiança e pelo carinho, espero que saibam que podem sempre contar comigo.

A toda a malta do Micro&Nano 14/15 pela união, pelas jantaradas e acima de tudo por terem partilhado estes cinco anos comigo, e saberem como ninguém as dificuldades que todos superámos.

A todos vocês obrigado!

Abstract

This work is focused on the investigation of a new mechanism for triplet harvesting in organic molecules, which is based on the energy transfer between triplet and singlet electronic states of different moieties.

Excited triplets are electronic states of multiplicity 1, which are not so enabled to contribute to the radiative process in organic molecules since the transition between the excited state and the ground state (a singlet state, with spin multiplicity 0) is spin-forbidden. Therefore, the lifetime of the triplet state is usually very long (μs or even ms time range) and triplets tend to lose their energy by non-radiative processes due to collisions with other molecules and vibrations. This fact is paramount for the performance of organic light emitting diodes (OLEDs). In the way OLEDs work, upon charge recombination, 75 % of the created excited states are dark triplets and only 25 % are emissive singlet states, hence the internal efficiency of the device is limited to 25 %. Mechanisms to harvest triplet states in organic materials are thus of great importance to improve device efficiencies.

Herein, a perylene bisimide unit of strong luminescence yield is used as the acceptor (A) for energy transfer from two thiophene derivatives used as energy donors (D) in a D-A-D molecular structure. The donor units form triplets in high yield once excited. However, the strong overlap between the phosphorescence of the donor and the S_0-S_1 absorption of the perylene promotes fast energy transfer from the triplet state of the donor to the singlet state of the perylene unit, from where emission occurs. In this way, triplets are harvested and become able to contribute to the emission. This novel, and often ignored mechanism is investigated in detail using steady-state and time-resolved luminescence spectroscopy techniques and applied in prototype OLEDs.

Keywords: Energy Transfer, Thermally Activated Delayed Fluorescence (TADF), Triplet harvesting, Organic Light-Emitting Diodes (OLEDs)

Resumo

Este trabalho apresenta um novo mecanismo de *triplet harvesting* em moléculas orgânicas baseado na transferência de energia entre estados eletrónicos de diferente multiplicidade de unidades covalentemente ligadas.

Estados *triplet* excitados são estados eletrónicos de multiplicidade 1 que não estão habilitados a contribuir para o processo radiativo de moléculas orgânicas, uma vez que a transição entre o estado excitado e o estado fundamental (estado *singlet*, multiplicidade 0) é proibida por spin. Como consequência, o tempo de vida do estado *triplet* é geralmente longo (µs ou até mesmo ms) e este tende a perder a sua energia através de processos não radiativos devido a colisões com outras moléculas e vibrações. Isto é relevante para a performance de díodos orgânicos emissores de luz (OLEDs). No modo de operação dos OLEDs, sobre recombinação de cargas, 75 % dos estados excitados criados são *triplets* não emissivos e apenas 25 % são estados *singlets* emissivos. Assim, mecanismos para o *harvesting* de estados *triplet* em materiais orgânicos são de elevada importância para melhorar a eficiência de dispositivos.

Nesta dissertação, uma unidade perilene bisimide de alto rendimento luminescente é usada como unidade aceitante (A) para a transferência de energia a partir de dois derivados de tiofene, usados como doadores (D) numa estrutura D-A-D. As unidades doadoras têm um rendimento elevado de formação de *triplets* quando excitadas, no entanto, a forte sobreposição entre a fosforescência do doador e a absorção da unidade perilene promove uma rápida transferência de energia do estado triplet do doador para o estado *singlet* da unidade aceitante, a partir da qual ocorre emissão. Deste modo, *triplets* são colhidos, tornando-se aptos para contribuir para a emissão. Este novo e geralmente ignorado mecanismo é investigado em detalhe nesta dissertação, recorrendo a técnicas de espectroscopia de estado estacionário e resolvida no tempo e aplicado a protótipos OLEDs.

Keywords: Transferência de Energia, *Thermally Activated Delayed Fluorescence* (TADF), *Triplet harvesting, Organic Light-Emitting Diodes* (OLEDs)

Abbreviations

A	Acceptor Unit
a.u.	Arbitrary Units
CT	Charge Transfer
D	Donor Unit
DCM	Dichloromethane
DF	Delayed Fluorescence
EBL	Electron Blocking Layer
EQE	External Quantum Efficiency
ETL	Electron Transport Layer
FRET	Förster Resonance Energy Transfer
HBL	Hole Blocking Layer
HOMO	Highest Occupied Molecular Orbital
HTL	Hole Transport Layer
IC	Internal Conversion
IRF	Instrument Response Function
ISC	Intersystem Crossing
ITO	Indium Tin Oxide
iCCD	Intensified charge-coupled device
LED	Light-emitting diode
LUMO	Lowest Unoccupied Molecular Orbital
mCP	(1,3-Bis(carbazol-9-yl)benzene)
OLED	Organic Light Emitting Diode
OXD-7	1,3-Bis[2-(4-tert -butylphenyl)-1,3,4-oxadiazo-5-yl]benzene
PF	Prompt Fluorescence
PH	Phosphorescence
PLQY	Photoluminescence Quantum Yield
PO-T2T	2,4,6-tris[3-(diphenylphosphinyl)phenyl]-1,3,5-triazine
PS	Polystyrene
RISC	Reverse Intersystem Crossing
SOC	Spin-Orbit Coupling
TADF	Thermally Activated Delayed Fluorescence
TCSPC	Time-Correlated Single Photon Counting
TPBi	2,2',2''-(1,3,5-Benzinetriyl)-tris(1-phenyl-1-H-benzimidazole)
TTA	Triplet-Triplet Annihilation
UV	Ultraviolet
VR	Vibrational relaxation

Symbols

ϵ	Extinction Coefficient
k	Constant Rate
τ	Lifetime
λ	Wavelength
Φ	Yield
n	Principal Quantum Number
l	Angular Quantum Number
m_l	Magnetic Quantum Number
m_s	Spin Quantum Number
S_0	Ground State
S_n	Singlet State
T_n	Triplet State
ΔE	Energy Gap
ΔE_{ST}	Singlet to Triplet Energy Gap

Table of contents

List of Figures

List of Tables

Chapter I. Motivation and Objectives

Light has a huge impact on human behaviour, and over the centuries, humanity has learned how to control it. During the 19th century, artificial light had several forms, from Murdoch's oil gas lamp to Hammer's compact fluorescent lamp, passing through the striking incandescent bulb of Thomas Edison. Light control went further in the 20th and 21st century with implementation in television, smartphones, as well as now in emerging applications.

The search for more economical and environment-friendly sources drives through light-emitting diodes (LED), which according to The United Nations Environment Programme doubles in performance every two years, decreasing in price by approximately 20 % every year. [1] From this efficient device arose the organic light-emitting diode (OLED), which nowadays is a hot topic due to their advantages over the LED by means of organic semiconductors characteristic features. However, the biggest drawback of OLED is its limited efficiency of 25 % due to spin's arrangement of the formed excitons. The research to overtake this drawback and achieve high-performance cost-effective devices brought the thermally activated delayed fluorescence (TADF) OLEDs, presented by Chihaya Adachi's group in 2011. [2] TADF molecules have been highly used as emitters having excellent performance in organic devices. Nevertheless, a huge possibility of molecular arrangements (small molecules, oligomers, polymers) will have an enormous impact in the next years, despite the great progress already made in the last decade. This will provide the improvements required for OLEDs in terms of efficiencies and lifetimes, to maximize their commercial potential and use in emerging applications.

The broad objective of this thesis is to contribute to this challenging topic presenting a novel triplet harvesting mechanism shown in a D-A-D structure composed of a perylene bisimide core coupled to thiophene units. Perylene bisimides is one of the most investigated compounds among polycyclic aromatic hydrocarbons during the last decade. Its intense absorption, fluorescence yields close to 100 %, photostability and good electron-acceptor behaviour became perylene bisimide a compound highly explored in the field of functional organic materials. When coupled to other structures is possible to acquire distinct photophysical properties enhancing the efficiency of a device. [3] Using thiophene-2 as a donor unit coupled to perylene bisimide is shown a new triplet energy harvesting mechanism, presented and discussed throughout this work. The mechanism goes beyond the TADF one and can become one important mechanism for OLEDs evolution since it allows larger flexibility in molecular design and narrower emission spectra since it does not require charge-transfer states.

This work is focused on exploring the photophysical properties of the ARC-1476 molecule in the context of its application in OLEDs.

Work Strategy

The present work was divided into three main stages:

i. Fundamental optical characterization: After preparation of the solution and solid-state samples these were optically characterized by steady-state spectroscopy collecting absorption, emission, and excitation spectra.

ii. Advanced Optical characterization: Dynamic processes were studied after the light incidence in the ARC-1476 molecule by means of time-resolved spectroscopy. The evolution of the emission was studied in a time-correlated single-photon counting setup in degassed and non-degassed solution and in an iCCD coupled setup in degassed solution and solid-state sample.

iii. Device fabrication and testing under operation: Fabrication of devices with 0.5 %, 1 % and 1.5 % of ARC-1476 as an emitting layer deposited by spin-coating method whilst the remaining layers were deposited by thermal evaporation. The fabrication was followed by electrical characterization of the devices.

Chapter II. Introduction

1. OLEDs: Challenges and Opportunities

Organic semiconductors are materials mostly constituted by carbon and hydrogen, which exhibit optical and electronic properties that are commonly found in inorganic semiconducting materials. These properties combined with the deposition by means of cost-effective printing methods, low-temperature and using environment-friendly processes transformed organic semiconductors on an appealing class of materials. [4]

In 1987, C. Tang and V. Slyke were pioneers with the development of the first organic-based light-emitting diode, and since then the era of organic optoelectronics started to grow significantly. [5] Nowadays, with the development of new device architectures, materials and mechanisms, organic light-emitting diodes (OLEDs) have become a hot-topic for emergent applications.

OLEDs are luminescence devices with an organic emissive layer that emits light in response to an electric stimulus. A voltage is applied to create a current of electrons that flows across the device and in the external circuit. Due to electrostatic forces, electrons and holes flow towards each other, recombine forming an exciton, which can either be a singlet or a triplet exciton, depending on the way spins of the recombined charges arrange. Assuming equal efficiency of charge recombination and neglecting external processes that may affect spin-statistics, 75 % will recombine in triplet states, which are mostly non-emissive (dark triplets) whilst the other 25 % will become singlet emissive states. The internal efficiency of these devices is thus limited to 25 %, that is the main drawback of OLEDs. [6], [7]

In order to achieve higher efficiencies, new mechanisms were proposed, and the pure organic fluorescent compounds were left behind towards compounds containing heavy metals. In 1998, the development of phosphorescent emitters significantly increased the efficiencies obtained but still, some problems remained unsolved. Metal complexes with emission in the blue region shows pronounced degradation devices, and the expensive use of metals may create environmental problems if used in the manufacture of devices with large output, such as displays or lightning industries. As a result of continuous research, in 2011 emerged a new generation of OLEDs. Launched by Adachi's group, the generation is based on thermally activated delayed fluorescence (TADF) mechanism, which will be further described in section 3. [2]

White and monochromatic TADF devices have already been achieved and the higher efficiencies were reached using single TADF emitters and exciplex states. [8]–[10] To date, the external quantum efficiencies (EQE) (ratio of extracted photons by injected charges) of these devices are ~30 % for both blue and green OLEDs, whilst red shows efficiencies of ~20 %. [11]–[13] The search for electroluminescent materials with emission out of the visible range is also one of the challenges. Near-Infrared (NIR) emitters have left behind the UV emitters due to their good stability and thus, device durability. Besides that the range of NIR emission coincides with the biological tissue semitransparency window, which also makes these devices interesting for applications in the biosensing and medical area. [14] These emitters are usually lanthanide-based or, transition metal-based, as for example in porphyrin-based materials. [15]–[18]

However, it is not just the emitter that is in constant research, for a good device efficiency ideal hosts are so important as the emitter to maximize the electroluminescence performance reducing the quenching. The relation between the host and the emitter is important and affects several parameters of the device such as external quantum efficiency, device lifetime, power efficiency, among others. Youtian Tao et al. (2011), presented the interpretation of using small organic molecules as host for phosphorescent OLEDs once they have precise molecular structures and can easily be purified, but the search for better results continued. [19] Exciplex and TADF materials already shown their performance as emitters and now a new application is getting the attention. Due to their charge transfer behaviour, Ziqi Wang et al. (2019) searched the possibility of use exciplex and TADF materials as hosts. [20]

OLEDs have attracted the interest of the academia as well as industrial sectors as a result of the characteristic features of organic materials as flexibility, low energy consumption, high contrast level, optical and electrical high performance. Multinational companies as Samsung®, Merck®, Novaled®, LG®, as well as many others have been working on the optimization of emitting materials and devices. Nowadays, these devices are already used in smartphones, displays, solid-state white lighting as well as in emerging applications, increasing the research around this topic. [21] According to IDTechEx research, smartphones dominate the OLED sector comprising around 81 % of the market revenue in 2018, but also televisions attract some of the attention representing the second-largest sector. [22]

2. Excited-state deactivation pathways

To achieve higher electroluminescence efficiencies, it is important to understand the photoluminescence mechanisms occurring in an organic system. Once a molecule is excited with light of a proper wavelength the transition from the ground state (S_0) to a state of higher energy with the same multiplicity is promoted. This transition is called absorption and is the starting point of all the other transitions. The excitation usually occurs to a higher vibrational level of the excited singlet state and fast relaxation to the lowest vibrational level of this state is promoted. The vibrational relaxation (VR) is then followed by internal conversion (IC) if the electron is in an excited state higher than S_1. As represented in Figure 1, also a transition from S_1 to an excited state of different multiplicity (T_1) can occur. The probability of this transition called intersystem crossing (ISC) depends on the singlet and triplet excited states involved but is usually low due to the difference in the spin multiplicity. [23], [24] The spin state flip is achieved by the spin-orbit coupling (SOC) interaction, which promotes phosphorescence emission. [6]

The above-mentioned processes are non-radiative, but also radiative decay can occur after excitation of a molecule. Fluorescence is the radiative decay that quickly (10^{-10} – 10^{-7} s) occurs from S_1, releasing the molecule's extra energy in the form of a photon. According to the Stokes Rule and to the Jablonski diagram represented in Figure 1, the wavelength of this emission is always longer than the absorption wavelength because of the energy loss due to vibrational relaxation thus, is easy to distinguish the absorption and fluorescence spectrum of a compound. [24], [25] In other hands, when the emission occurs from a state with different multiplicity of S_0 is called phosphorescence. Unlike the previous decay, this one is not an instantaneous emission due to the "forbidden" transitions involved and has a characteristic time of 10^{-6} – 1 s and must compete with non-radiative de-excitation at room

temperature. The phosphorescence spectrum appears at longer wavelengths than the fluorescence spectrum due to its lower energy. [26] In competition with phosphorescence is also the reverse intersystem crossing (RISC) where triplets are up-converted to a high energy singlet excited state. However, RISC is possible only in molecules that have a small energy difference between S_1 and T_1, for which the thermal energy must be enough to overcome the barrier. [27], [28]

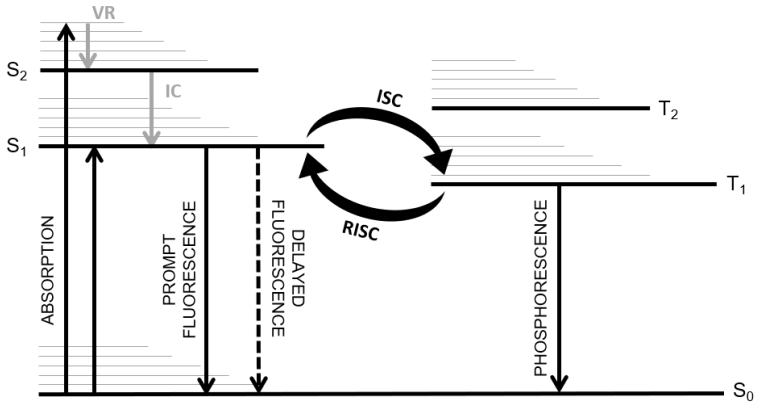

Figure 1. Jablonski diagram. Adapted from [24] and [29]. VR, vibrational relaxation; IC, Internal Conversion; ISC, Intersystem Crossing; RISC, Reverse Intersystem Crossing.

3. Triplet harvesting mechanisms

Triplet harvesting mechanisms are of vital importance to achieve more efficient OLEDs and several ways to harvest triplet excited states have been developed. Delayed fluorescence and room temperature phosphorescence are the main ways from which triplet states are known to be involved in the radiative process. Delayed fluorescence can be assigned to triplet-triplet annihilation (TTA) or thermally activated delayed fluorescence (TADF) however, the TADF mechanism overshadowed the TTA mechanism because the design of efficient TTA systems is complex, and excellent results have been already obtained with TADF systems. [30]

3.1. Room-temperature phosphorescence

The presence of heavy atoms as iridium (Ir) and platinum (Pt) in organic systems led to room temperature phosphorescence with lifetimes shorter than the typical ones for pure organic phosphorescent material and high photoluminescence quantum yields, increasing the internal device efficiencies by the strong spin-orbit coupling (SOC) interactions, which are influenced by the atomic number of the material. The SOC induces mixing of singlet and triplet excited states and thus allows the coupling of T_1 to S_0, electronic states of different multiplicities, turning the spin-forbidden processes into allowed transitions. [31], [32] Fluorescence is usually not observed in these organo-metallic complexes because it cannot compete with the fast intersystem crossing rate (k_{ISC}). Upon the formation of a singlet excited state, the intersystem crossing efficiently populates the long-lived state from where the complex emits as phosphorescence. [33], [34]

Despite the good results obtained with these materials, covering nearly the whole visible spectrum, the use of heavy metal-based complexes leads to high device fabrication costs and is not compatible

with some research areas that use emission to study and detect species and interactions, as in the biosensors area.

3.2. Thermally activated delayed fluorescence

Thermally activated delayed fluorescence mechanism is operative in molecules where the thermal energy is enough to up-convert triplet states to the emissive singlet manifold by reverse intersystem crossing, happening due to the low energy difference between the singlet and triplet states (ΔE_{ST}), generally lower than 0.2 eV. [35]

In a way to reduce the energy difference between the excited states of different spins, it is important to consider the exchange energy, which affects the two states due to electron-electron repulsion imposed by Pauli's principle. The exchange energy value is connected with the overlap of the spatial wavefunction of the HOMO and LUMO and thus can be minimized decreasing this overlap. [36] The presence of charge transfer (CT) states is the main way used to minimize HOMO-LUMO overlap and thus reduce ΔE_{ST}, facilitating reverse intersystem crossing. The acceleration of the ISC and RISC rates is promoted by mixing the CT states with triplet states of more localized character and thus promoting an efficient triplet harvesting. Dias's and co-workers studied several TADF molecules based on CT states with external quantum efficiencies close to 100 % obtained by triplet exciton harvesting. [37]–[39]

The photophysical characterization of TADF molecules is largely facilitated when the contribution of delayed fluorescence is large. [30], [33], [40] In this case triplet formation yield can be easily determined by the relation between the delayed fluorescence and the total emission of the emitter ($\phi_{PF}+\phi_{DF}$), according to Equation 1.

$$\phi_{ISC}=\frac{\phi_{DF}}{\phi_{PF}+\phi_{DF}} \quad (1)$$

In these TADF molecules the rate of reverse intersystem crossing, following an Arrhenius type law, must be faster when compared to the rate of the non-radiative decays that affect the triplet states. [24], [30] The RISC rate constant can easily be described considering the lifetime of the delayed fluorescence, and both prompt (ϕ_{PF}) and delayed fluorescence (ϕ_{DF}) yields, according to the Equation 2.

$$k_{rISC}=\frac{1}{\tau_{DF}}\left(\frac{\phi_{PF}+\phi_{DF}}{\phi_{PF}}\right) \quad (2)$$

The TADF mechanism is significant when a very high yield of singlet states formed by RISC is involved. Therefore, the RISC rate needs to be faster than the deactivation pathways of the triplet state so, the gap between T_1 and S_0 as to be large in a way to suppress the non-radiative decay from T_1, increasing the possibility of up-conversion. The RISC efficiency is given by Equation 3 and is approximately 1 in molecules where the suppression of non-radiative decay from the triplet state occurs.

$$\phi_{rISC}=\frac{k_{rISC}}{k_{rISC}+k_{IC}^{T}+k_{PH}} \quad (3)$$

In order to increase the efficiency of TADF emitters, new strategies are still in study as well as the improvement of already existing strategies, considering all the important mechanisms occurring upon excitation of a molecule.

4. A New Mechanism Based on D-A structures: Energy Transfer

Molecules can transfer their excess energy to other molecules by means of a long-range dipole-dipole interaction describing the Forster mechanism or by a short-range mechanism (Dexter). [41], [42]

Forster resonance energy transfer (FRET) is a mechanism where the donor molecule (D) is initially in its electronic excited state and transfers energy to another molecule, referred as the acceptor (A), initially in the ground state, through a non-radiative dipole-dipole coupling. This interaction occurs in a distance range of 10 – 100 Å. [43], [44] In contrast, the Dexter transfer mechanism is only operative at much shorter distances (< 10 Å). The Dexter mechanism involves the hopping of an electron transferring an exciton from D to A. For this to happen it is important that wavefunction of D overlaps the acceptor's wavefunction. [41], [42]

4.1. The molecule ARC-1476

The molecule presented in Figure 2 has a structure composed by an acceptor unit covalently linked to donor units presenting a D-A-D structure. The acceptor unit is a perylene derivative. Perylene ($C_{20}H_{12}$) is composed of two naphthalene molecules attached by a C-C bond at the positions 1 and 8 forming a rigid polycyclic aromatic hydrocarbon. Perylene has shown great photophysical properties, which increased their use as a fluorescent dye and, the emergence of perylene derivatives has become noticeable in optoelectronic applications. [45] The perylene derivative used as acceptor on the molecule ARC-1476 is the perylene polycyclic aromatic scaffold substituted with piperidine-2,6-dione at the 3,4- and 9,10- positions known as perylene bisimide (3,4,9,10 - Perylenetetracarboxylic). [45], [46] Perylene bisimide has an intense absorption and strong luminescence yield demonstrating exceptional optical properties. In addition, its high mobility, accepting ability and photostability are also reasons of the increasing applications using this perylene derivative, as organic electronics and photovoltaic devices, fluorescence spectroscopy, control of light-matter interactions in photonic devices and biomolecular imaging. [47], [48]

The two donor units are thiophene derivatives already studied by Joana Jõgela et al. [49] covalently linked at the *peri* position as an extension along the molecular axis. This individual molecule shows absorption in the UV region and emits blue fluorescence. [50] These molecules form triplet states in high yield once excited that are harvested and thus, can contribute to the overall emission.

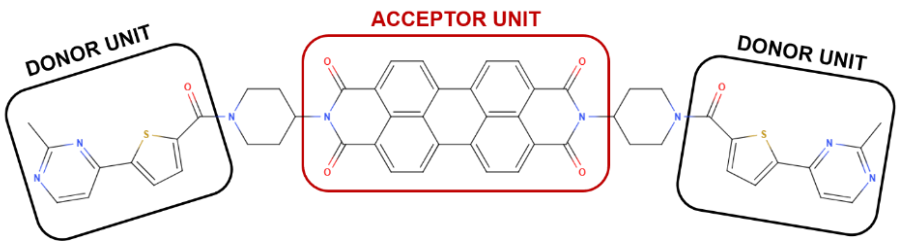

Figure 2. Molecular structure of ARC-1476.

The molecule studied throughout this work was produced by Erki Enkvist and Asko Uri from the University of Tartu, Estonia, and later sent to the Physics Department of Durham University for photophysical studies and devices fabrication using the molecule as emitting layer dopant.

Chapter III. Experimental Methods

The main experimental apparatus and techniques used in this work are described in this chapter. In section A of Appendices are presented supplementary information about the solvent and used hosts.

1. Sample preparation

For all photophysical studies, two different samples were used: solution and solid-state samples. For solution samples, a known mass of ARC-1476 was dissolved in chloroform obtaining a molar concentration of 10^{-5} M, after the total material dissolution was then transferred to a quartz cuvette to proceed with the measurements presented on the following topics.

Solid-state samples were produced by drop-casting. These samples required previous preparation of proper solutions once small molecules do not form good thin films due to their low molecular weight. In order to avoid quenching of the emission and get better thin film quality, polystyrene was used as host once it is an inert polymer. Solutions for deposition were obtained mixing the ARC-1476 solution and the polystyrene solution such that the mass concentration of the polystyrene solution was one hundred times greater than the ARC-1476 solution. Ratios of 1 %, 0.5 %, 0.1 %, 0.05 %, 0.01 % and 0.005 % by mass were studied. With a pipette, 70 µL of the solution was dropped covering the whole surface of the substrate and was heated at 60 °C to accelerate the solvent evaporation, forming a thin film.

2. Steady-State Spectroscopy

Absorption spectra is an important measure that provides the absorption regions of the molecule allowing a more accurate excitation choice for all the measurements needed. To obtain absorption spectra was used a Shimadzu UV-3600 double beam spectrophotometer collecting between 245 nm (chloroform cut-off wavelength) and 700 nm with a 0.5 nm step in the solution. Steady-state emission spectra were collected in a FluoroLog fluorometer from Horiba Scientific. Different excitation wavelengths were applied according to the absorption spectra with 1 nm incremental step and an integration time of 0.3 s. Excitation spectra were collected with the same parameters as emission spectra and using emission wavelengths according to the emission peak values.

3. Time-Resolved Spectroscopy

Solution sample was first studied in a time-correlated single-photon counting (TCSPC) Deltaflex Lifetime Fluorometer from JY Horiba, which allows measuring lifetimes from 25 ps to 1 s, coupled to a SpectraLED S-330 excitation source. [51] In order to study the influence of oxygen on the emission, both degassed and non-degassed solutions were studied under the same parameters. The degassed solution was obtained by freeze-pump-thaw cycling method. The solution was placed in a proper cuvette and connected to a vacuum pump, which evacuated the headspace above the sample after the frizzing step. The frizzing and evacuation steps were repeated five times to ensure higher gas removal.

A degassed solution was also used to determine the emission as a function of power with the sample placed inside a Janis Research Company Inc. cryostat, under vacuum. It was necessary to use a low-

temperature cuvette that is fitted with a long glass tube to fit the dimensions of the cryostat. In this measurement, the emission was collected by a JY-190 spectrograph and imaged by an intensified charge-coupled device (iCCD) camera (Stanford Computer Optics 4 Picos) with an excitation wavelength of 337 nm provided by an NML 100 N_2 pulsed laser with a 3 ns pulse width and a repetition rate of 10 Hz (Setup in Section B of Appendices). The luminescence intensity was collected over a specified integration time after a previously specified delay time. To control the power dose applied the setup was coupled with a chopper and a power supply controller to exponentially increase the power. The same study was carried for the 0.005 % solid-state sample.

For temperature dependence measurements, the solid-state sample was lowered from 295 K to 80 K using liquid nitrogen and an electrical temperature controller, Lake Shore 331, with a stabilization period of 20 min at each temperature, so that the temperature would be uniform throughout the whole cryostat.

Measurements using an excitation wavelength of 355 nm and 532 nm were performed with a Nd:YAG pulsed laser working at 10 Hz repetition rate, with 150 ps pulse width.

4. Electrochemical characterization

Charge transfer processes are the main processes involved in OLEDs and therefore the electrochemical response of the ARC-1476 in solution was evaluated by cyclic voltammetry using an electrolyte composed by tetrafluoroborate (BF^4) and dichloromethane in a 0.1 M concentration. It was used a molar concentration of 1 mM of ARC-1476 in DCM. Ferrocene was used as the standard in a concentration smaller than 10 mM. Supplementary information is presented in section C of Appendices.

5. Photoluminescence quantum yield determination

The determination of photoluminescence quantum yield (PLQY) in solution was performed using fluorescein as standard. This method is based on the comparison of the photoluminescence efficiency of ARC-1476 in chloroform against the efficiency of fluorescein in 0.1 M NaOH. [52]

The determination of PLQY in solid-state was based on the method proposed by Greenham et al., using the home-built setup presented in Figure 3. [53] Three measurements, direct and indirect excitation, and empty integration sphere was recorded to determine the PLQY using a constant excitation source, collecting the photoluminescence spectra. Measurements were performed using an integration sphere coupled with a sensitive QePro spectrometer (Ocean Optics) using 453 nm LED light source.

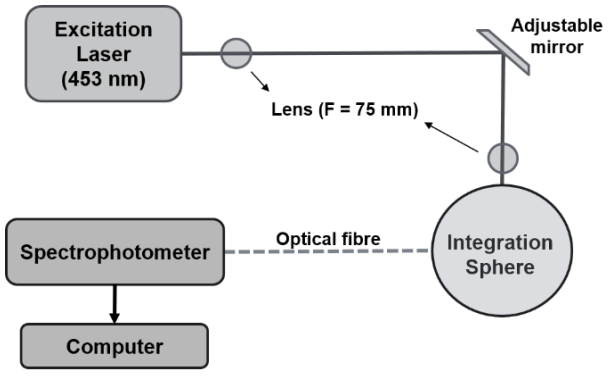

Figure 3. Photoluminescence quantum yield experimental scheme.

The PLQY determination was performed using three measurements, however, it is enough to record only two measurements, direct excitation and empty integration sphere. For a more accurate value, the third measurement was performed with indirect excitation of the sample to consider the possibility of reabsorption of the emitted light.

After collecting the data for the sample dispersed in polystyrene, Equations 4, 5 and 6 were used for PLQY determination.

$$\Phi_X = \frac{P_D}{L_E - L_D} \quad (4)$$

$$\Phi_X = \frac{P_D - (1 - A)\, P_I}{L_E\, A} \quad (5)$$

$$A = 1 - \frac{L_D}{L_I} \quad (6)$$

Where A is the sample absorbance, L is the integral intensity of direct excitation (L_D), indirect excitation (L_I), and empty integration sphere (L_E) and P is the integral photoluminescence intensity of direct excitation (P_D) and indirect excitation (P_I).

6. Devices' production

Starting from a solution with a concentration of 0.5 mg/mL of ARC-1476 in pure chloroform, different vials were prepared with the volume needed to evaporate and obtain the necessary amounts of compound to produce devices with 0.5 %, 1 % and 1.5 % of ARC-1476 in the emitting layer.

As referred in sample preparation topic, a host is needed to improve the thin film quality and thus, it was used a mixture of hosts to produce two types of devices, TADF and non-TADF exciplex hosted devices. The TADF exciplex hosted devices were produced using a blend of 80 % of mCP and 20 % of PO-T2T in volume, while the blend in non-TADF devices was 70 % of mCP and 30 % of OXD-7, both exciplex hosts were dissolved in an azeotropic mixture of 95 % of chloroform and 5 % of chlorobenzene in volume to achieve better film deposition by spin-coating.

Patterned ITO glass substrates were cleaned with acetone and dried to eliminate large impurities, then the substrates were put in an acetone ultrasound bath for 15 minutes followed by an equal step with isopropyl alcohol. After the cleaning step, a square with a thickness of 20 nm of molybdenum trioxide was deposited by thermal evaporation in a Lesker automated system and then the emitter was spin-coated over the MoO_3. The substrate was fixed in the spinner by vacuum suction and using a pipette, 70 µL of solution were deposited to cover whole substrate spinning it at 5000 rpm during 60 s. This was followed by a drying step at 60 °C in order to remove any solvent in excess.

The electron transport layer (ETL) of the devices is one of the main differences, the TADF device has PO-T2T as ETL while TPBi is used on non-TADF devices but both were deposited by thermal evaporation in the system mentioned before and present a thickness of 50 nm. The two bottom layers, lithium fluoride, and aluminium were both thermally evaporated achieving thicknesses of 0.7 nm and 100 nm respectively, obtaining the following structures (Figure 4):

- **ITO** | **MoO_3** (20 nm) | mCP:PO-T2T (80:20) co x % **ARC-1476** (60 nm) | **PO-T2T** (50 nm) | **LiF** (0.7 nm) | **Al** (100 nm)
- **ITO** | **MoO_3** (20 nm) | mCP:OXD-7 (70:30) co x % **ARC-1476** (60 nm) | **TPBi** (50 nm) | **LiF** (0.7 nm) | **Al** (100 nm)

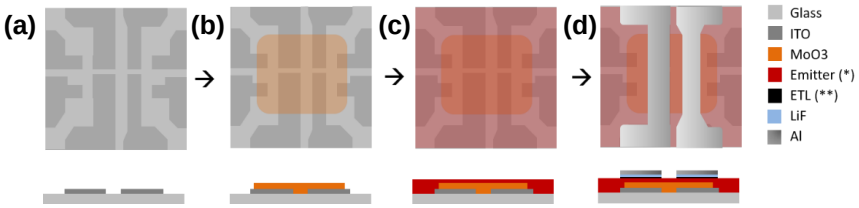

Figure 4. Schematic of layers deposition. **(a)** Patterned ITO glass substrate. **(b)** Molybdenum trioxide deposition by thermal evaporation. **(c)** Emitting layer deposition by spin-coating *(*) Device 1: mCP:PO-T2T (80:20) co x % ARC-1476; Device 2: mCP:OXD-7 (70:30) co x % ARC-1476*. **(d)** ETL *(**) Device 1: PO-T2T; Device 2: TPBi*; lithium fluoride and aluminium deposition by thermal evaporation.

7. Devices' characterization

Non-encapsulated devices were characterized at room temperature right after the last evaporation process. Each device was placed in an integration sphere LMS-100 Labsphere that was connected to a Keithley source meter 2425 model and an Ocean Optics USB4000 Spectrometer.

Chapter IV. Results and Discussion

In this chapter, the results obtained throughout the work are presented and discussed. Starting from the photophysical characterization of the ARC-1476 molecule, which consists of advanced photophysical and complementary characterization, followed by its incorporation into devices and their optical and electrical study.

1. Fundamental optical photophysics

1.1. Steady-state photophysics

The ARC-1476 presents low solubility in most of the organic solvents, being negligible in alcohols, ethers, and water. Even though the addition of phenol helps to increase solubility, this substance acts like a quenching agent and deactivates the emission. By virtue of the strong emission from the ARC-1476 in chloroform, this was the solvent used in all the measurements, even though presenting only moderate solubility (~0.5 – 2 mg/mL). Additional information about this solvent can be consulted on Section A of Appendices.

Figure 5 (a) shows the normalised absorption and steady-state fluorescence spectra of the ARC-1476 compound and Figure 5 (b) shows the absorption, fluorescence and phosphorescence of the individual donor unit.

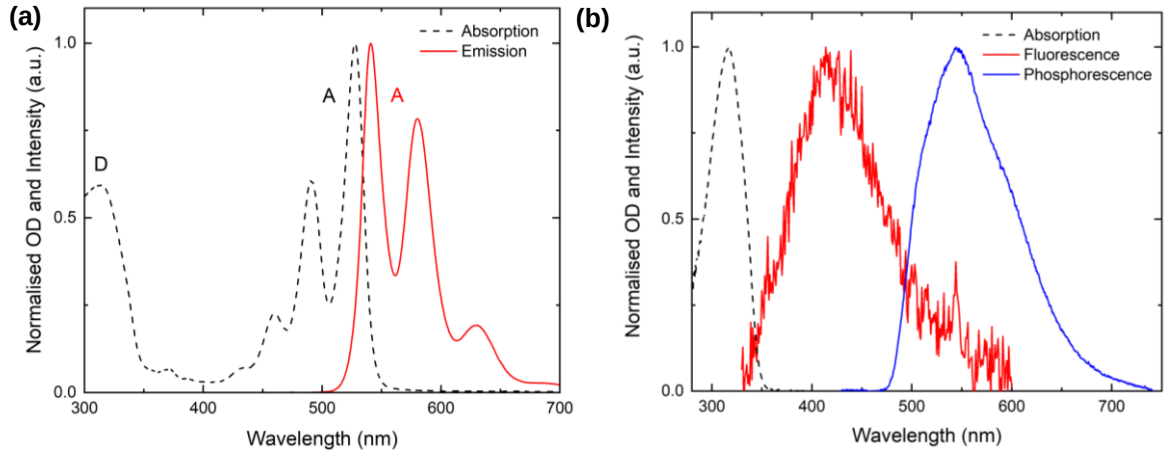

Figure 5. (a) Absorption (Dashed) and Photoluminescence (Red) spectra of ARC-1476 in chloroform, λ_{ex} = 325 nm. (b) Absorption (Dashed), fluorescence emission (Red) spectra of the donor in chloroform, λ_{ex} = 325 nm. Phosphorescence spectrum (Blue) of the donor dispersed in polystyrene at 80 K, λ_{ex} = 337 nm.

By comparing the spectra in Figure 5 (a) and Figure 5 (b) it becomes clear that the absorption of ARC-1476 is composed by a broadband observed at short wavelengths, which is due to the absorption of the single donor unit, and by a well-resolved band observed at relative longer wavelengths due to the absorption of perylene bisimide unit, which is used as the energy acceptor unit in the ARC-1476 compound. The perylene bisimide emission is well known in the literature, being easily recognized in Figure 5 (a). [3] The first absorption band, λ_{max} = 313 nm is assigned to π-π* transitions of the donor and the three following bands, λ_{max} = 460 nm, λ_{max} = 491 nm and λ_{max} = 527 nm are all attributed to the acceptor unit. Smaller peaks are also visible in the absorption spectrum of the complex at λ_{max} = 371

nm and λ_{max} = 433 nm and are also assigned to the perylene bisimide acceptor. This is in accordance with the excitation spectra obtained with emission collected in the acceptor region, given in Figure 6 (b), which mimics the absorption spectrum.

The photoluminescence spectrum in solution shows a well-resolved structure characteristic of perylene derivatives with emission maxima at 541 nm, 580 nm and 630 nm. [3], [45], [46] It is noteworthy that the ARC-1476 emission resembles the acceptor emission when 325 nm is used to excite the sample.

As seen in Figure 6 (a), the emissions of the separated units and of the compound are consistent with an energy transfer mechanism, but not with the occurrence of charge transfer (CT). The emission of the ARC-1476 compound matches the peak values of the acceptor emission. This indicates clearly that no charge transfer is taking place between the D and A units. The excited state of CT D-A-D structures usually presents a Gaussian emission shape, which is shifted when compared to the emission of the separated D and A units. Moreover, emission from states of charge-transfer character is usually accompanied by a shift to longer wavelengths with increasing solvent polarity due to redistribution of the electronic density associated with charge-transfer dipole. [33], [40] Clearly this not happening here. In ARC-1476, once the light is absorbed in the donor unit region, the emission of the complex coincides with the emission of the acceptor unit. Moreover, the ARC-1476 excitation spectrum obtained with emission collected in the acceptor region shows contribution of both D and A absorptions. This shows that the D is able to transfer its excited state energy to the acceptor unit. The fact that no D emission is observed, also shows that the energy transfer mechanism occurs with high efficiency. It is noteworthy that both the fluorescence and phosphorescence of the D unit overlap strongly the absorption of the A unit, thus the conditions that promote efficient energy transfer between both units are entirely satisfied.

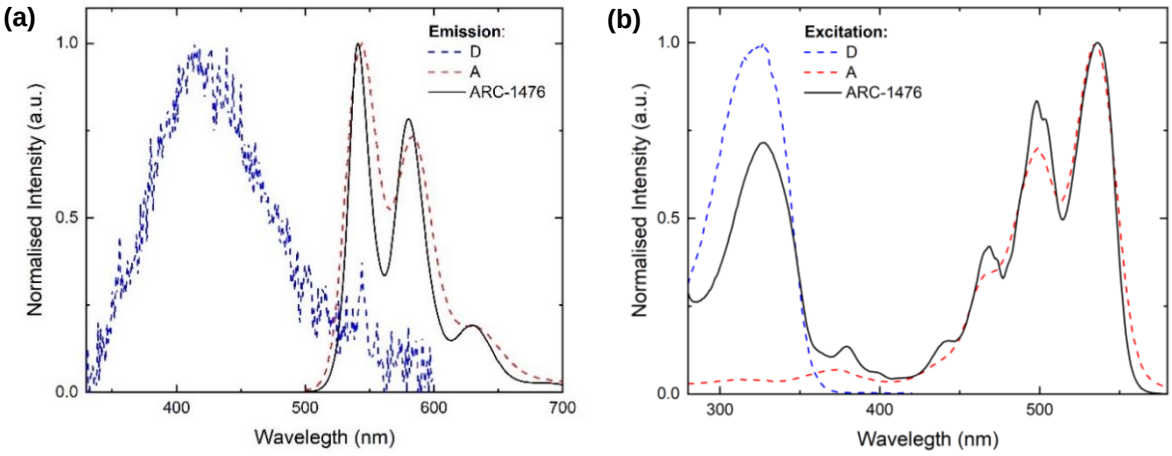

Figure 6. Normalised (a) emission and (b) excitation spectra of the donor (thiophene-2), acceptor (perylene bisimide) and ARC-1476 in chloroform.

The energy of the emissive singlet excited state S_1 is determined from the onset of the fluorescence spectrum for the donor and acceptor units. This emission band corresponds to the transition between S_1 and S_0. Similarly, the energy of the triplet excited state T_1 is determined from the onset of the phosphorescence spectrum. Therefore, using Figure 5 (a) it is possible to obtain the values of S_1 of the acceptor, whilst S_1 and T_1 of the donor is taken from Figure 5 (b). The following values were obtained from emission onsets: S_1^D = 3.8 eV, T_1^D = 2.6 eV, S_1^A = 2.4 eV. Owing to the strong overlap between

the fluorescence of the singlet D unit and the absorption of the A unit singlet-singlet energy transfer should be active. However, it might be that because the phosphorescence of the D unit also overlaps the absorption of the acceptor unit that triplet to singlet energy transfer may also be operative. In this case, the fluorescence of the acceptor would show a delayed component decaying in the microsecond or millisecond time range that will be observed only when the D unit is excited. As the gap between the donor singlet excited state and the acceptor triplet state is of 0.2 eV, with the triplet state of the donor unit being above the emissive singlet state of the acceptor, the energy transfer occurring between T_1^D and S_1^A will be a downhill process, showing no energy barrier. The investigation of this potential mechanism for triplet harvesting is the focus of the work reported in this thesis.

1.2. Absorption extinction coefficient

The Beer-Lambert's law states that the absorption of light in a solution, defined as the logarithm of the ratio between the intensities of the incident and transmitted beams is proportional to the beam path and concentration of the solution at a given wavelength. The proportionality constant $\epsilon(\lambda)$, is the molar absorptivity (e.g. extinction coefficient) and is expressed in units of $mol^{-1} \cdot L \cdot cm^{-1}$. The concentration of the solution can thus be determined by measuring the absorption once the molar absorptivity is known.

In order to determine the molar absorptivity of the molecular compound, the absorbance (A) of a solution containing the molecule is measured at a single wavelength and plotted against the solution concentration (c). According to Beer-Lambert's law, the dependence of the absorbance with concentration should vary linearly, and the molar absorptivity $\epsilon(\lambda)$ is determined directly from the slope. [54]

Figure 7 (a) shows the absorption spectra of the ARC-1476 obtained for different concentrations in chloroform all of them with absorbances bellow 1 to avoid effects that may lead to deviations from the linearity. The absorption at 490 nm is represented in Figure 7 (b) against the solution concentration, showing a clear linear dependence as expected. Using a linear fitting, the slope is determined, giving a molar absorptivity of 52 000 $M^{-1} \cdot L \cdot cm^{-1}$ at 490 nm. This absorptivity indicates a strongly allowed electronic transition between π-π* orbitals, from the ground state S_0 to S_1.

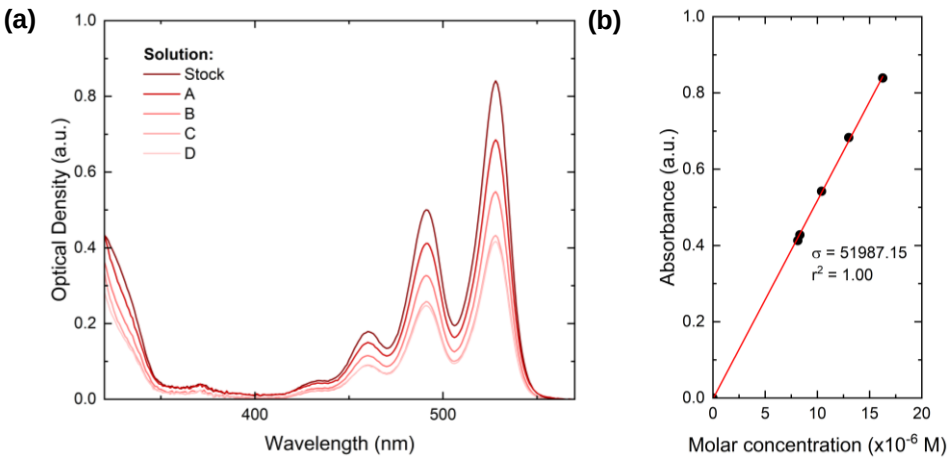

Figure 7. (a) Absorption spectra of five ARC-1476 chloroform solutions with different and known concentrations. (b) Absorbance at 490 nm vs Molar concentration linear fit.

1.3. Photoluminescence Quantum Yields

The photoluminescence quantum yield (PLQY) measures the efficiency of the radiative process in a molecule, following excitation. In this work, the PLQY was determined using fluorescein as the standard, which has a known quantum yield of 0.79 in solution, with an emission range of 500 – 600 nm, similar to the ARC-1476 emission. [55] The method used is based on recording fluorescence emission of the compound and of the fluorescein standard, obtained at a specific excitation wavelength. Solutions with different absorbances are used and the integral of the emission spectrum is represented as a function of absorbance. Figure 8 represents the relation between the integrated emission, obtained from the fluorescence emission spectra collected with an excitation wavelength of 490 nm (acceptor excitation for the complex) and solution absorbance. A clear linear relationship is observed in both the complex ARC-1476 and the fluorescein standard. The slopes obtained from the linear fit in each graph are related with the PLQYs of both the fluorescein (ϕ_S) and the complex ARC-1476 (ϕ_X) by Equation 7. [55] The absorption and fluorescence emission spectra used for the elaboration of the graphs represented in Figure 8 are provided in section D of Appendices.

$$\Phi_X = \Phi_S \frac{Grad_X}{Grad_S} \frac{\eta_X^2}{\eta_S^2} \quad (7)$$

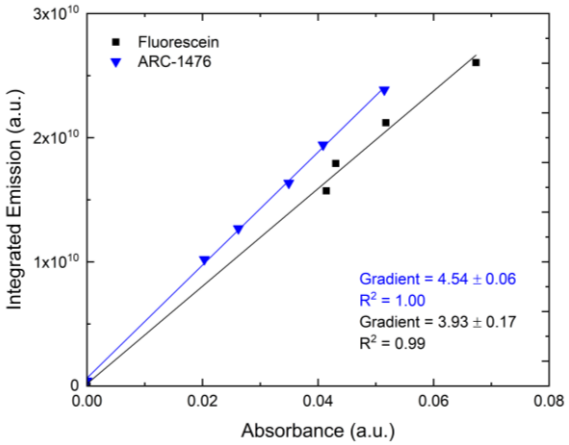

Figure 8. Linear fit of fluorescein (Black), used as standard and ARC-1476 (Blue).

Directly from observation of Figure 8 is possible to conclude that the complex ARC-1476 has a PLQY higher than fluorescein. However, since different solvents were used in the solutions of both compounds, it was necessary to consider the refractive indices of the solvents in Equation 7. The η_X is the refractive index of chloroform, which takes the value of 1.45 and η_S is equal to 1.34, the value of the refractive index of the sodium hydroxide (NaOH) aqueous solution. Substitution of the values in Equation 7 gives a PLQY close to 1. This is in clear agreement with previous PLQY values determined for perylene bisimide, and basically reflects the slow rates of deactivation through non-radiative processes in this perylene derivative, which cannot compete with the radiative rate. [46]

The determination of the photoluminescence quantum yield of ARC-1476 in solid-state was performed in drop-cast films, prepared with 0.005 % of the compound dispersed in polystyrene, giving a PLQY of 31 ± 6 %. The reason for using such low concentration is due to the fact that ARC-1476 tends to strongly aggregate in solid films and shows strong luminescence quenching. [56]

The difference between the photoluminescence quantum yield in solution and in a solid thin film is significative but justified by the different behaviour of the molecule in solution and thin film. The PLQY in solution is high, indicating that intramolecular quenching plays no important role, this means, internal conversion and intersystem crossing are not affecting the fluorescence decay. However, in the solid thin film, the luminescence is quenched significantly, decreasing to 31 % at very low concentration, and decreasing further if the concentration is increased, most probably because of aggregate formation involving π-π* stacking of perylene moieties. [24], [29]

2. Time-resolved photoluminescence study

2.1. Time-Correlated Single Photon Counting

Figure 9 shows the time-resolved fluorescence decay of ARC-1476 following laser excitation at 330 nm (excitation at the donor unit) for both degassed (black) and non-degassed (blue) solutions.

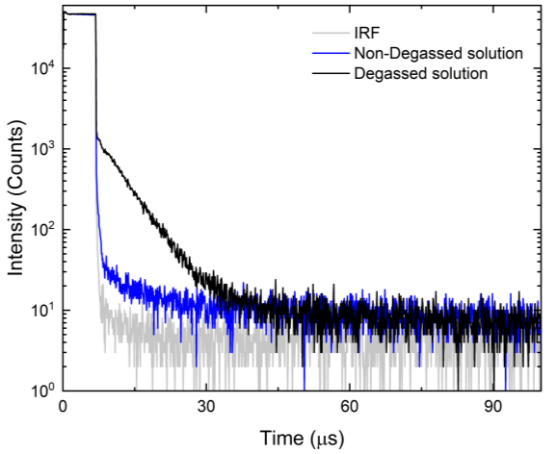

Figure 9. Transient photoluminescence decay of ARC-1476 in solution. λ_{ex} = 330 nm

The difference observed between the decay of fluorescence in non-degassed and degassed solutions reflect the contribution of delayed fluorescence due to energy transfer from the donor unit to the perylene bisimide acceptor and is evidently remarkable. When oxygen is present, dissolved in the solution, triplet states in the donor are unable to transfer their energy to the acceptor singlet emissive states, due to the strong quench of the triplet population caused by the collision with oxygen molecules. Oxygen exists as a triplet in its ground state, therefore, when oxygen molecules collide with the ARC-1476 molecules, energy transfer from the triplet state of ARC-1476 to oxygen is promoted. This mechanism deactivates the triplet states that could contribute to delayed fluorescence. Therefore, the contribution of delayed fluorescence is practically absent in the presence of oxygen. [57] In non-degassed solutions only a small delayed fluorescence component is observed decaying with a supposed lifetime of 0.4 μs, which is probably associated with the slow turn-off of the excitation source and is not part of the fluorescence emission of the ARC-1476 compound. Once oxygen is removed a pronounced increase in delayed fluorescence intensity is observed, decaying with a lifetime of 6.1 μs.

2.2. Time-resolved gated measurements

Time-gated spectroscopy offers advantages over time-correlated single-photon counting, which does not follow direct changes in the photoluminescence spectrum. The working principle of time-gated cameras is based on the image intensifier and a more detailed procedure can be consulted on Section B of Appendices.

According to the study previously done by J. Jõgela et al., thiophene-2 is a phosphorescent donor that reveals moderate room temperature phosphorescence with an emission peak at 560 nm. [49] This is in clear agreement with the phosphorescence spectrum of the donor unit, given in Figure 5 (b). To further investigate the emissive response of the individual donor unit, spectroscopic studies were performed and a phosphorescence emission with a lifetime of 69.6 ± 0.7 ms was obtained, described by a monoexponential fit, as shown in Section E of Appendices.

The time-resolved fluorescence decay of ARC-1476 given in Figure 10 shows two clearly distinct components, one decaying in the nano-second time regime that is attributed to the decay of directly formed singlet states in the perylene acceptor (either by direct excitation or rapid singlet-singlet energy transfer from the D to the A unit), and a long-lived component, decaying in the microsecond time range that is attributed to the decay of perylene singlet states formed by energy transfer from the triplet state of the donor unit. Confirming this interpretation, the fluorescence decay of ARC-1476 can only be fitted by the sum of two exponentials. One first exponential decaying with a lifetime of 4.9 ± 0.4 ns assigned to the prompt fluorescence – i.e. fluorescence attributed to directly excited singlet states in the perylene moiety, or eventually formed by fast singlet-singlet energy transfer from the donor to the acceptor unit – followed by a long-lived delayed fluorescence component with a 5.7 ± 0.9 µs lifetime, in good agreement with the value obtained from the donor triplet state.

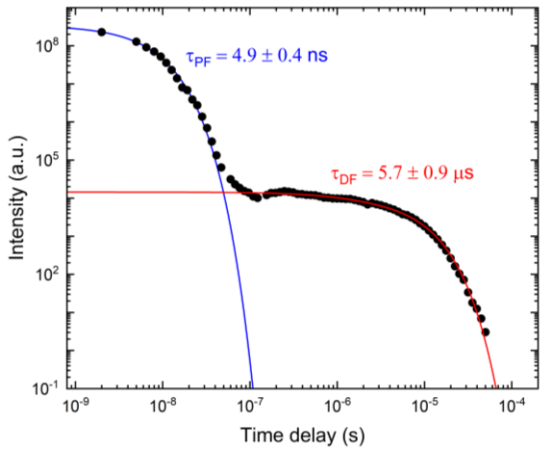

Figure 10. Time-resolved fluorescence decay curve of ARC-1476 in solution at room temperature. λ_{ex} = 337 nm

The interpretation of the ARC-1476 fluorescence decay is further confirmed by performing time-gated fluorescence decays using excitation on the donor unit (λ_x = 355 nm), and directly on the acceptor (λ_x = 532 nm). Figure 11 shows the decays of ARC-1476 fluorescence obtained upon excitation on the donor and on the acceptor. As expected, and in contrast with the decays obtained with excitation on the donor unit, when the acceptor is excited directly, no delayed fluorescence is observed, and the emission decays with a lifetime of 1.6 ± 0.1 ns.

When the D-A-D structure is excited with the 355 nm laser the donor singlet excited state is first populated. However, the fluorescence emission that is observed is that of the acceptor. This is due to the energy transfer mechanism occurring between the donor and acceptor units. This energy transfer involves two initial competing steps: the donor singlet excited states can either decay to the ground-state giving origin to donor fluorescence (not observed) or can be rapidly transferred to the singlet excited state of the acceptor unit, from where they decay radiatively giving origin to perylene fluorescence that decays with 4.9 ns lifetime. Competing with these two steps is the intersystem crossing rate that converts singlet excited states into triplet states of the donor unit. This process is very efficient in the thiophene derivative used as the donor unit. [49] Once the triplet states of the donor are formed, they can be transferred to the singlet state of the perylene acceptor, giving origin to the delayed fluorescence observed decaying with a lifetime around 6 μs.

When the acceptor unit is directly excited no energy transfer takes place and all the excited donor states decay with the prompt fluorescence lifetime, i.e., no delayed component is observed.

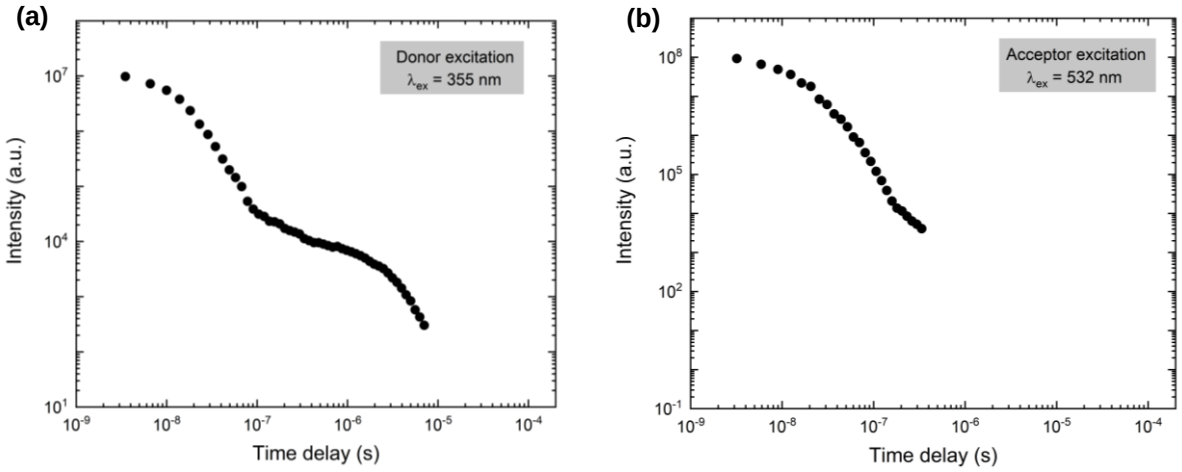

Figure 11. Time-resolved fluorescence decay curves of ARC-1476 dispersed in polystyrene upon (a) donor and (b) acceptor excitation in vacuum at room temperature. Excitation wavelengths 335 nm and 532 nm were used in this experiment, respectively.

The relative contributions of prompt and delayed fluorescence can be determined from the decay represented in Figure 10 using the Equation 8, where A_{PF} and A_{DF} represent the pre-exponential amplitudes associated with the prompt and delayed fluorescence decays, respectively. τ_{PF} and τ_{DF} are the prompt and delayed fluorescence lifetimes.

$$\frac{\int DF}{\int PF} = \frac{A_{DF}\tau_{DF}}{A_{PF}\tau_{PF}} \quad (8)$$

Using Equation 8 a ratio of 5.8 % is obtained for ARC-1476. The yield of perylene singlet states formed via the triplet to singlet energy transfer path is thus approximately 6 %, and according to Equation 9, this yield is equal to the product between the triplet formation yield in ARC-1476 – i.e. when the donor is in presence of the acceptor unit – $\Phi_T^{D/A}$ and the yield of energy transfer between the triplet state of the donor and the singlet state of the acceptor $\Phi_{ET}^{D^T\text{-}A^S}$.

$$\frac{\int DF}{\int PF} = \frac{\Phi_T^{D/A} \cdot \Phi_{ET}^{D^T\text{-}A^S} \cdot \Phi_f^A}{\Phi_f^A} = \Phi_T^{D/A} \cdot \Phi_{ET}^{D^T\text{-}A^S} \quad (9)$$

The relative small yield of perylene singlet excited states formed via the triplet-to-singlet energy transfer path, just ~6 %, when compared with the prompt fluorescence contribution, ~94 %, strongly indicates that the rate of singlet-singlet energy transfer from the donor to the acceptor unit is much faster than the rate of intersystem crossing of the donor unit. Therefore, the triplet formation yield in the complex is very small and most probably be the step that limits the efficiency of the mechanism (under optical excitation). If the donor triplet state population is formed in great numbers, for example via electrical excitation, then the yield of perylene singlet states formed via the triplet-to-singlet energy transfer will be much larger. This is potentially the situation in devices, where triplet formation yields close to 75 % are expected to occur.

Figure 12 shows the time evolution of the ARC-1476 emission spectra, i.e. real time-resolved spectra obtained at different delay times following excitation, obtained with excitation in the donor and with excitation in the acceptor unit. In agreement with the time-resolved decay curves (Figure 10), prompt and delayed fluorescence components are detected. Very importantly, both the prompt and delayed fluorescence components show the same perylene-like emission spectrum, fully confirming the mechanism that has been described above and is represented in Figure 13.

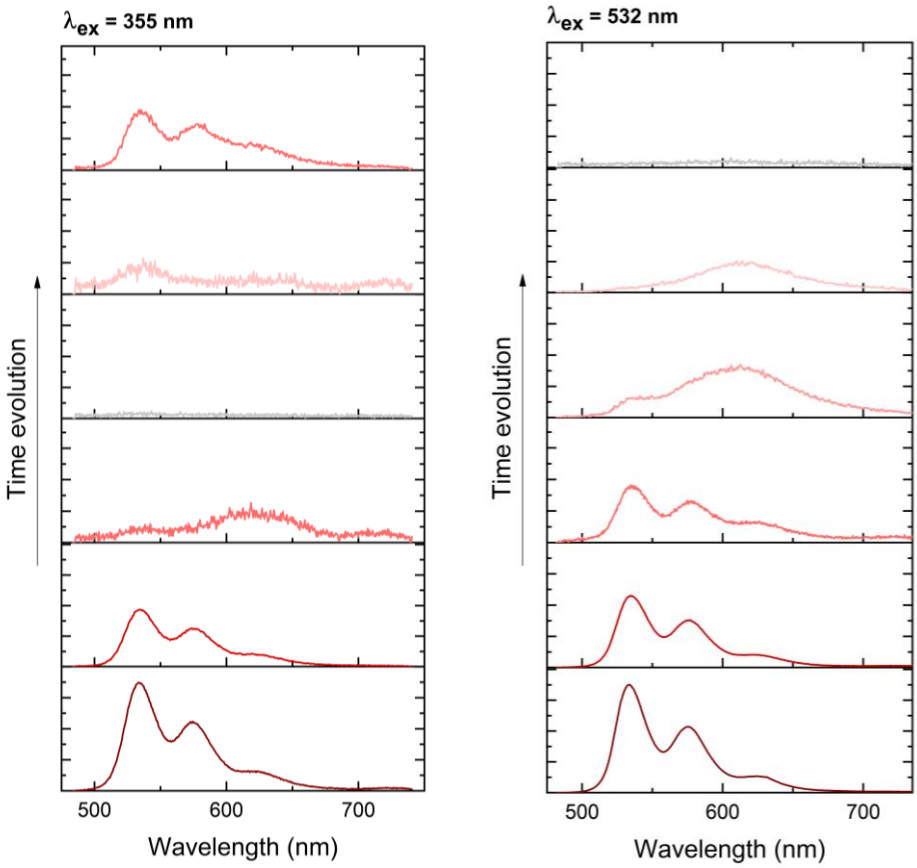

Figure 12. Representation of the intensity overtime for an excitation wavelength of 335 nm and 532 nm. For this representation was used real data but it is important to notice that intensity amplitudes are not at scale.

In both cases, i.e. either with 355 nm or 532 nm excitation, a weak broad emission following the decay of the prompt fluorescence (50 ns delay time) appears. This is possibly due to the formation of aggregate species, as it is well known that perylene derivatives are affected by significative aggregation in solid-state. [3], [46]

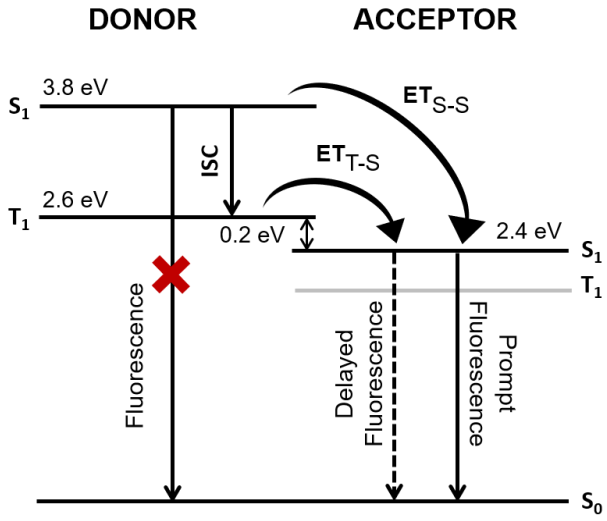

Figure 13. Schematic of the Triplet-to-Singlet energy transfer mechanism occurring upon donor excitation.

2.3. Power Dependence

Delayed fluorescence can be originated in response to different mechanisms. For example, the annihilation of triplet excited states (TTA), caused by biomolecular collisions of two excited triplet states has a probability of creating a singlet excited state, which can then release its energy in the form of fluorescence. Similarly, the up-conversion of triplet excited states to the singlet manifold via a thermally activated reverse intersystem crossing process also creates delayed fluorescence. The two mechanisms can be distinguished by the variation of the delayed fluorescence intensity with excitation dose. [58], [59]

The variation of the delayed fluorescence with the excitation dose on intermolecular mechanisms (as in TTA) occurs due to the competition between the rate of monomolecular decay of the triplet states ($k_{PH}+k^{T}_{IC}$) and the rate for diffusion-controlled collisions (k_{TTA}). This competition is described by a quadratic response, in other words, when plotted the integrated emission versus excitation dose in a logarithmic scale, presents a gradient equal to 2. In contrast, the intramolecular mechanism (as in TADF molecules) assumes a gradient equal to 1, representing a linear dependence upon excitation dose. [30]

The triplet-to-singlet energy transfer mechanism that is responsible for the delayed fluorescence in ARC-1476 is of intramolecular origin. The intensity of the delayed fluorescence should then vary linearly with excitation dose. This is confirmed in Figure 14 showing a perfect linear dependence (gradient 1 in a log-log scale) of the delayed fluorescence intensity with excitation power, for both in chloroform solution (10^{-5} M) and when ARC-1476 is dispersed in polystyrene (drop-casted solid-state sample with 0.005 %).

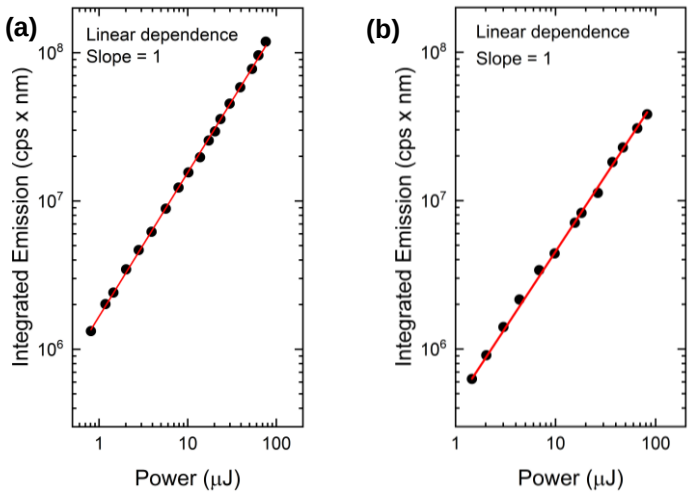

Figure 14. Power dependence of ARC-1476 delayed fluorescence in (a) chloroform solution and (b) 0.005 % dispersed in polystyrene at room temperature.

2.4. Temperature Dependence

Figure 15 shows the variation of ARC-1476 fluorescence decay with temperature in the interval from 80 K to 295 K.

No significant variation with temperature is observed in the entire temperature interval. Given the energy alignment shown in Figure 13, this is expected as the triplet-to-singlet energy transfer occurs downhill, so with no significant energy barrier. Moreover, perylene with PLQY close to the unit is also expected to show no variation of fluorescence intensity with temperature. The temperature variation of ARC-1476 fluorescence is thus entirely consistent with the mechanism described in Figure 13. [3], [39], [60], [61]

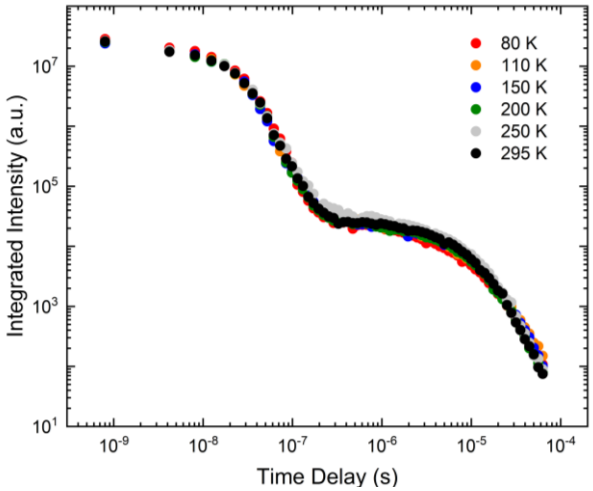

Figure 15. Time-resolved fluorescence decay of the thin-film sample at different temperatures, varying between 80 K and 295 K. λ_{ex} = 337 nm.

3. Electrochemistry

Cyclic voltammetry is one of the most useful characterization methods that allow the estimation of the energy band diagram of the compound. The ionization potential (IP) and electron affinity (EA) of the molecule are determined accordingly with Equation 10 and 11, respectively.

The IP is related to the extraction of one electron from the molecule, implying an oxidation process. Its energy value was estimated by the empirical Bredas relation for the ionization potential, given in Equation 10. [62]

$$IP = - [E_P + 4.8 - E_{1/2}] \quad (10)$$

In other hands, the EA involves a reduction process, reflecting the energy needed to add an electron in the molecule, given by Equation 11, electron affinity. [62]

$$EA = - [E_N + 4.8 - E_{1/2}] \quad (11)$$

From the voltammogram disclosed in Figure 16, performed at 0.05 $V \cdot s^{-1}$ scan rate, it was possible to determine the oxidation (E_P) and reduction (E_N) potentials of the ARC-1476 complex.

In both equations, $E_{1/2}$ is relative to the standard potential of the ferrocene redox pair (Fc/Fc^+), assuming a value equal to 0.03 V.

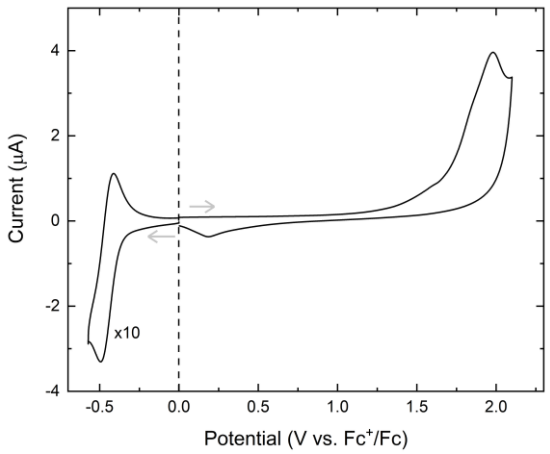

Figure 16. Cyclic voltammetry showing electrochemical processes of ARC-1476.

Hence, from the electrochemical reduction and oxidation onset potentials were estimated the energies associated with the IP and EA, also commonly referred as the HOMO and LUMO energies, which take the values of IP = E_{HOMO} = - 6.4 eV and EA = E_{LUMO} = - 4.4 eV. As a result, the electrochemical energy gap was found to be 1.99 eV.

The very deep HOMO of ARC-1476 makes hole injection difficult in devices using indium tin oxide (ITO) electrodes due to the large energy barrier (1.7 eV) created between the ARC-1476 complex and ITO, which presents a work-function of 4.7 eV.

4. Devices

Organic light-emitting diodes using the ARC-1476 compound as the dopant were fabricated using a solution processing method. The poor solubility of ARC-1476 and its tendency to form non-emissive aggregates limited the range of concentrations used to 0.5 %, 1.0 %, and 1.5 %. Additional layers were used as described in Figure 17, in order to maximize charge recombination in the emissive layer (More details in Chapter III). Holes and electrons are confined in the emitting layer due to the energy barriers created by the MoO_3 and mCP layers.

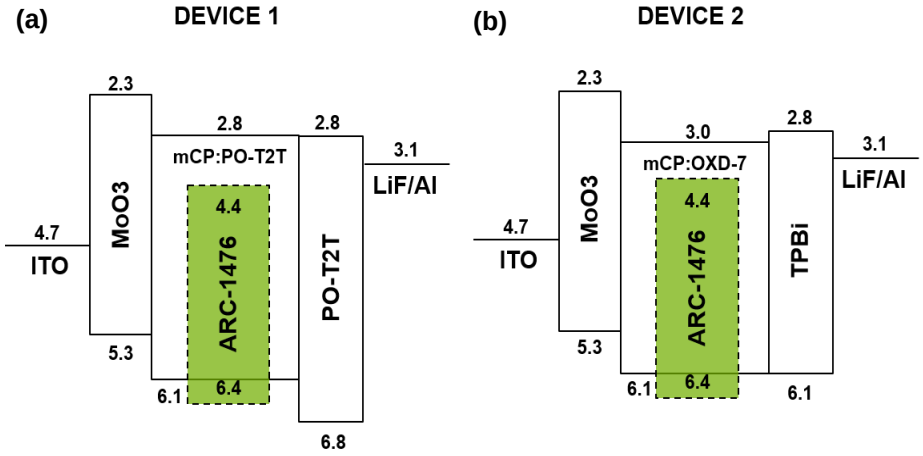

Figure 17. Schematic of (a) device 1 and (b) device 2, with the respective HOMO and LUMO values (eV).

Both structures present a top electrode of aluminium with a layer of lithium fluoride to improve the electron injection capability to the organic material, for a better electron transport a layer of PO-T2T in the device 1 and a layer of TPBi in the device 2 were introduced. Molybdenum trioxide layer works as a hole injection and electron blocking layer to help to increase the number of charges in the organic emitting layer and promote charge recombination. Structures were deposited in a glass substrate patterned with ITO, which works as the anode. The choice of the used hosts was based on the HOMO and LUMO levels of the ARC-1476, which present values of 6.4 eV and 4.4 eV, respectively.

The two types of devices (1 and 2) with a concentration of 1.5 % were characterized and the results are shown in Figure 18 and Figure 19.

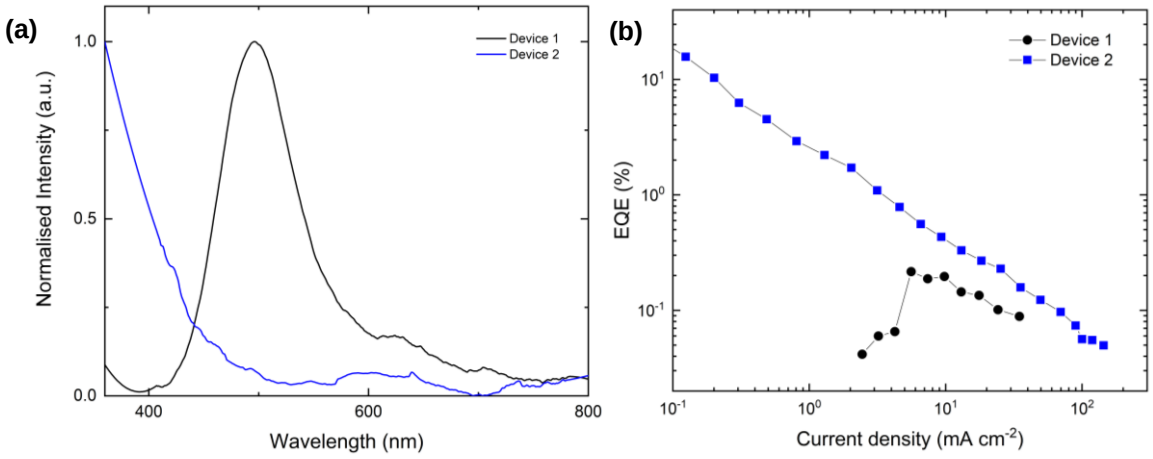

Figure 18. Characteristics of OLED devices 1 and 2 using the ARC-1476 as the emitter. (a) Electroluminescence spectra (b) External quantum efficiency (EQE) vs. current density.

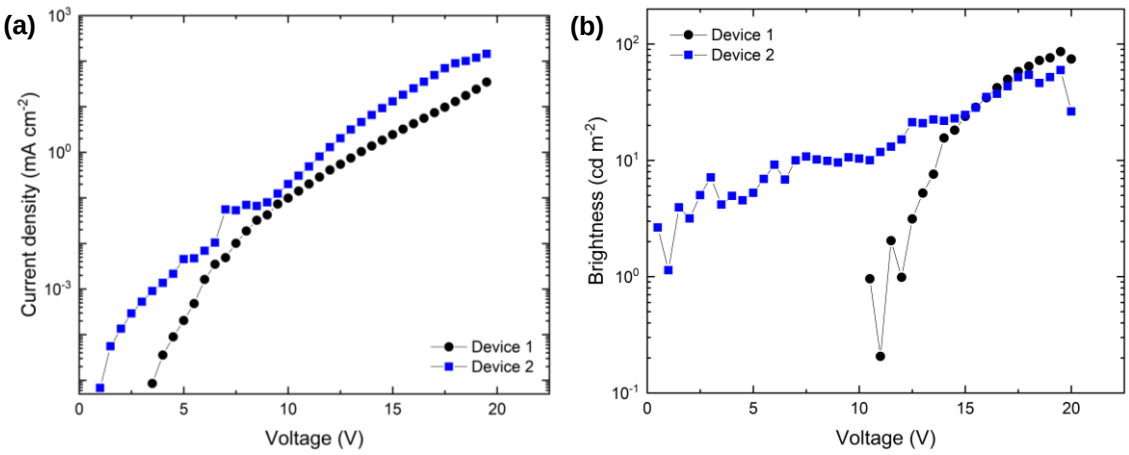

Figure 19. Characteristics of OLED devices 1 and 2 using the ARC-1476 as the emitter. (a) J-V curves; (b) Brightness vs. potential.

Unfortunately, the performance of ARC-1476 devices is poor. In both devices, the electroluminescence spectra are significantly different when compared with the photoluminescence spectrum. This is particularly evident for device 2. However, even in device 1, a significant blue shift is observed in the electroluminescence when compared to the photoluminescence. The low concentration of ARC-1476 used in the devices is part of the problem, as much charge recombination occurs in the host instead of occurring in the ARC-1476 molecules. However, the weaker emission from the host in device 1 indicates that energy transfer from the host to ARC-1476 is occurring. It is known from the literature that mCP:PO-T2T blend, used as host in device 1, is an efficient TADF blue-emitter with a photoluminescence quantum yield of 55 % and an EQE of 16 %. Therefore, if no significant energy transfer occurred, host electroluminescence should have been observed. [63], [64] The lack of strong electroluminescence from ARC-1476 should due to the strong luminescence quenching affecting ARC-1476 in the solid-state.

The turn-on voltage of device 1 is 3.5 V, which is in the range of an OLED structure using a layer of mCP:PO-T2T. Device 2 shows a smaller turn-on voltage of 1 V, that is consistent with the energy alignment, that promotes charge confinements in the emissive organic layer. [65]

Despite the data obtained, the aim of acquiring organic light-emitting diodes with emission from the ARC-1476 dopant was not achieved. Different deposition methods could be a way to avoid the aggregation of the material allowing the use of higher concentrations and thus, better device efficiencies may be achieved.

Chapter V. Conclusions and future perspectives

The photophysical study of the D-A-D structure composed by a perylene bisimide as acceptor unit and two thiophene derivative donor units, referred as ARC-1476 led to the investigation of a new mechanism for triplet harvesting in organic molecules based on the energy transfer between triplet and singlet electronic excited states of different moieties (D and A) covalently linked. The perylene bisimide unit is the entity responsible for the (prompt and delayed) fluorescence emission, even upon donor excitation, presenting a maximum emission peak at 541 nm.

The energy transfer mechanism involves initial intersystem crossing (ISC) between the singlet and triplet states of the donor unit, occurring in competition with the fast energy transfer between the singlet states of D and A. The ISC is followed by barrierless (0.2 eV) triplet to singlet energy transfer from the donor to the acceptor unit (T_1^D to S_1^A), promoted by the overlap between the phosphorescence of the thiophene and the absorption of the perylene bisimide. As a result of this process delayed perylene bisimide fluorescence is observed with a yield of 5.8 %, showing that triplets are being harvested.

Triplet harvesting mechanisms are paramount to increase the 25 % limited OLEDs efficiency, using the 75 % dark triplets produced it is possible to reach values close to 100 %. The mechanism presented in this dissertation brings a new way to harness the triplet excited states and thus, contribute to more efficient devices. The mechanism is in some ways analogous to TADF (thermally activated delayed fluorescence) but not involving charge transfer states, and thus allowing the observation of narrower emission spectra and larger flexibility in molecular design. These features bring advantages such as higher colour purity due to the narrower emission and lead researchers to think and look at possible new molecules in another way.

With the data obtained and studied throughout this work is not possible to assign the energy transfer mechanism to dipole-dipole coupling or electron exchange. As referred in Chapter II, the main difference between FRET and Dexter energy transfer mechanism is the length scale, whilst FRET is a long-distance mechanism occurring between 10 Å and 100 Å, Dexter mechanism occurs at distances less than 10 Å. [21], [41], [42] In the future, it is important to determine which mechanism is involved, changing the separation distance of the moieties.

Devices fabricated using the ARC-1476 compound as a dopant (0.5 %, 1.0 % and 1.5 %) of the emitting layer has shown weak performance due to the limitation on concentration imposed by the aggregation of the molecules thus, were not attained efficient devices with an emission peak at 541 nm. Despite the contribution of the triplet-to-singlet energy transfer mechanism, the used concentrations were not enough to supply the emission. The visible emission produced in both TADF and non-TADF exciplex hosted devices was mainly produced by the host. The aggregation problem is common in perylene derivatives and one possible way to achieve better device efficiencies passes by changing the deposition method. The emitting layer was deposited by spin-coating, which required low concentrations to decrease the probability of agglomerates once it is a solution-processed method, using vacuum thermal evaporation it is possible to achieve higher concentrations without this concern. Another approach to eliminating the aggregation promoted by the perylene derivative and thus, improve the

efficiency of devices using triplet to singlet energy transfer mechanism would pass by the choice of a different acceptor unit. [3], [46], [56]

The very deep HOMO of ARC-1476 (6.4 eV) is also a problem in the devices. With this value, the choice of hosts is more restricted, and the use of ITO is not suitable due to the large energy barrier created between the ARC-1476 complex and the anode. [66]

Concluding, the goal of this work was achieved with the study of a new triplet harvesting mechanism based on triplet-to-singlet energy transfer, however, like any other, the mechanism here presented requires improvements and continuous research to better understand each system.

Furthermore, some of the photophysical results here presented were published in a poster section at the *13th International Conference on Optical Probes of Organic and Hybrid Optoelectronic Materials and Applications*, in *Vilnius, Lithuania* (7-12th July 2019). The poster is presented in section G of Appendices.

The research around this new mechanism can lead to efficient results, bringing a possible alternative to TADF systems.

References

[1] Global Environment Facility and UNEP, “The rapid transition to energy efficient-lighting: An integrated policy approach,” *The United Nations Environment Programme*, 2013.

[2] A. Endo *et al.*, “Efficient up-conversion of triplet excitons into a singlet state and its application for organic light emitting diodes,” *Applied Physics Letters*, 2011.

[3] F. Würthner, “Progress in the synthesis of perylene bisimide dyes,” *Organic Chemistry Frontiers*, 2019.

[4] A. Schöll and F. Schreiber, “Thin films of organic molecules: Interfaces and epitaxial growth,” *Molecular Beam Epitaxy*, 2013.

[5] S. Slyke, C. Tang, “Organic electroluminescent diodes,” *Applied Physics Letters*, 1987.

[6] P. K. Samanta, D. Kim, V. Coropceanu, and J. L. Brédas, “Up-Conversion Intersystem Crossing Rates in Organic Emitters for Thermally Activated Delayed Fluorescence: Impact of the Nature of Singlet vs Triplet Excited States,” *Journal of the American Chemical Society*, 2017.

[7] U. Giovanella, M. Pasini, and C. Botta, *Organic Light-Emitting Diodes (OLEDs): Working Principles and Device Technology*. 2016.

[8] D. Graves, V. Jankus, F. B. Dias, and A. Monkman, “Photophysical Investigation of the Thermally Activated Delayed Emission from Films of m-MTDATA : PBD Exciplex,” *Advanced Functional Materials*, 2014.

[9] K. Goushi, K. Yoshida, K. Sato, and C. Adachi, “Organic light-emitting diodes employing efficient reverse intersystem crossing for triplet-to-singlet state conversion,” *Nature Photonics*, 2012.

[10] T. Higuchi, H. Nakanotani, and C. Adachi, “High Efficiency White Organic Light-Emitting Diodes Based on a Blue Thermally Activated Delayed Fluorescent Emitter Combined with Green and Red Fluorescent Emitters,” *Advanced Materials*, 2015.

[11] T. Lin, T. Chatterjee, W. Tsai, W. Lee, M. Wu, and M. Jiao, “Sky-Blue Organic Light-Emitting Diode with 37 % External Quantum Efficiency Using Thermally Activated Delayed Fluorescence from Spiroacridine-Triazine Hybrid,” *Advanced Materials*, 2016.

[12] J. Chen, K. Wang, C. Zheng, M. Zhang, Y. Shi, and S. Tao, “Red Organic Light-Emitting Diode with External Quantum Efficiency beyond 20 % Based on a Novel Thermally Activated Delayed Fluorescence Emitter,” *Advanced Science*, 2018.

[13] K. Pan *et al.*, “Efficient and Tunable Thermally Activated Delayed Fluorescence Emitters Having Orientation-Adjustable CN-Substituted Pyridine and Pyrimidine Acceptor Units,” *Advanced Functional Materials*, 2016.

[14] A. Zampetti, A. Minotto, and F. Cacialli, “Near-Infrared (NIR) Organic Light-Emitting Diodes (OLEDs): Challenges and Opportunities,” *Advanced Functional Materials*, 2019.

[15] A. Shahalizad *et al.*, “Enhanced near-infrared electroluminescence from a neodymium complex in organic light-emitting diodes with a solution-processed exciplex host,” *Applied Physics Letters*, 2019.

[16] L. Huang, C. D. Park, T. Fleetham, and J. Li, “Platinum (II) azatetrabenzoporphyrins for near-infrared organic light emitting diodes,” *Applied Physics Letters*, 2016.

[17] K. Tuong Ly *et al.*, “Near-infrared organic light-emitting diodes with very high external quantum

efficiency and radiance," *Nature Photonics*, 2017.

[18] C. L. Ho, H. Li, and W. Y. Wong, "Red to near-infrared organometallic phosphorescent dyes for OLED applications," *Journal of Organometallic Chemistry*, 2014.

[19] Y. Tao, C. Yang, and J. Qin, "Organic host materials for phosphorescent organic light-emitting diodes," *Royal Society of Chemistry*, pp. 2943–2970, 2011.

[20] Z. Wang, C. Wang, H. Zhang, Z. Liu, B. Zhao, and W. Li, "The application of charge transfer host based exciplex and thermally activated delayed fluorescence materials in organic light-emitting diodes," *Elsevier: Organic Electronics*, 2019.

[21] M. Colella, P. Pander, D. de S. Pereira, and A. P. Monkman, "Interfacial TADF Exciplex as a Tool to Localize Excitons, Improve Efficiency, and Increase OLED Lifetime," *ACS applied materials & interfaces*, 2018.

[22] R. Das, Ghaffarzadef Khasha, and X. He, "Flexible & Foldable OLED Displays 2019-2029," 2019.

[23] M. A. Omary and H. H. Patterson, *Encyclopedia of Spectroscopy and Spectrometry*, 3rd ed. Elsevier Ltd., 2016.

[24] B. Valeur, *Molecular Fluorescence*. 2009.

[25] A. T. R. Willams, *An Introduction to Fluorescence Spectroscopy*. 1981.

[26] N. Thejo Kalyani and S. J. Dhoble, "Organic light emitting diodes: Energy saving lighting technology - A review," *Renewable and Sustainable Energy Reviews*, 2012.

[27] T. Sato, R. Hayashi, N. Haruta, and Y. J. Pu, "Fluorescence via Reverse Intersystem Crossing from Higher Triplet States in a Bisanthracene Derivative," *Scientific Reports*, 2017.

[28] D. Hu, L. Yao, B. Yang, and Y. Ma, "Reverse intersystem crossing from upper triplet levels to excited singlet: A 'hot excition' path for organic light-emitting diodes," *The Royal Society: Mathematical, Physical and Engineering Sciences*, 2015.

[29] J. R. Lakowicz, *Principles of fluorescence spectroscopy*. 2006.

[30] F. B. Dias, T. J. Penfold, M. N. Berberan-Santos, and A. P. Monkman, "Photophysics of Thermally Activated Delayed Fluorescence in Organic Molecules," *IOP Science*, 2018.

[31] T. J. Penfold, E. Gindensperger, C. Daniel, and C. M. Marian, "Spin-Vibronic Mechanism for Intersystem Crossing," *Chemical Reviews*, 2018.

[32] C. Cebrián and M. Mauro, "Recent advances in phosphorescent platinum complexes for organic light-emitting diodes," *Beilstein Journal of Organic Chemistry*, 2018.

[33] C. Chen *et al.*, "Intramolecular Charge Transfer Controls Switching Between Room Temperature Phosphorescence and Thermally Activated Delayed Fluorescence," *Angewandte Chemie - International Edition*, 2018.

[34] P. Pander, A. Swist, J. Soloducho, and F. B. Dias, "Room temperature phosphorescence lifetime and spectrum tuning of substituted thianthrenes," *Elsevier*, 2017.

[35] A. Pershin *et al.*, "Energy in thermally activated delayed fluorescent molecules," *Nature Communications*, 2019.

[36] T. Hosokai *et al.*, "Evidence and mechanism of efficient thermally activated delayed fluorescence promoted by delocalized excited states," *Science Advances*, 2017.

[37] Z. Li *et al.*, "Modulation of Thermally Activated Delayed Fluorescence in Waterborne

Polyurethanes via Charge-Transfer Effect," *Chemistry - An Asian Journal*, 2019.

[38] P. Pander *et al.*, "Thermally activated delayed fluorescence with a narrow emission spectrum and organic room temperature phosphorescence by controlling spin-orbit coupling and phosphorescence lifetime of metal-free organic molecules," *Journal of Materials Chemistry C*, 2018.

[39] F. B. Dias *et al.*, "Triplet harvesting with 100% efficiency by way of thermally activated delayed fluorescence in charge transfer OLED emitters," *Advanced Materials*, 2013.

[40] F. B. Dias *et al.*, "The role of local triplet excited states and D-A relative orientation in thermally activated delayed fluorescence: Photophysics and devices," *Advanced Science*, 2016.

[41] S. S. Skourtis, C. Liu, P. Antoniou, A. M. Virshup, and D. N. Beratan, "Dexter energy transfer pathways," 2016.

[42] P. Taylor, A. Olaya-castro, and G. D. Scholes, "Energy transfer from Forster–Dexter theory to quantum coherent light-harvesting," 2011.

[43] F. Strieth-kalthoff, M. J. James, M. Teders, L. Pitzer, and F. Glorius, "Energy transfer catalysis mediated by visible light: principles, applications, directions," 2018.

[44] A. Kirch, M. Gmelch, and S. Reineke, "Resonance Energy Transfer from a Single Donor Material Simultaneous Singlet-Singlet and Triplet-Singlet Förster Resonance Energy Transfer from a Single Donor Material," *The Journal of Physical Chemistry*, 2019.

[45] C. Huang, S. Barlow, and S. R. Marder, "Perylene-3,4,9,10-tetracarboxylic acid diimides: Synthesis, physical properties, and use in organic electronics," *Journal of Organic Chemistry*, 2011.

[46] F. Würthner, C. R. Saha-Möller, B. Fimmel, S. Ogi, P. Leowanawat, and D. Schmidt, "Perylene Bisimide Dye Assemblies as Archetype Functional Supramolecular Materials," *Chemical Reviews*, 2016.

[47] R. Gronheid *et al.*, "Reversible intramolecular electron transfer at the single-molecule level," *Angewandte Chemie - International Edition*, 2003.

[48] S. Betzold *et al.*, "Tunable Light-Matter Hybridization in Open Organic Microcavities," *ACS Photonics*, 2018.

[49] J. Jõgela, A. Uri, L. O. Pålsson, and E. Enkvist, "Almost complete radiationless energy transfer from excited triplet state of a dim phosphor to a covalently linked adjacent fluorescent dye in purely organic tandem luminophores doped into PVA matrix," *Journal of Materials Chemistry C*, 2019.

[50] E. Enkvist *et al.*, "Protein-Induced Long Lifetime Luminescence of Nonmetal Probes," *ACS Chemical biology*, 2011.

[51] HORIBA UK, "SpectraLED," 2019. [Online]. Available: https://www.horiba.com/en_en/products/detail/action/show/Product/spectraled-1095/. [Accessed: 06-Sep-2019].

[52] G. A. Crosby and J. N. Demas, "Measurement of photoluminescence quantum yields. Review," *The Journal of Physical Chemistry*, 1971.

[53] N. C. Greenham *et al.*, "Measurement of absolute photoluminescence quantum efficiencies in

conjugated polymers," *Chemical Physics Letters*, 1995.

[54] T. Resource, "Extinction Coefficients: A guide to understanding extinction coefficients, with emphasis on spectrophotometric determination of protein concentration," *Pierce Biotechnology*, 2002.

[55] Jobin Yvon, "A Guide to Recording Fluorescence Quantum Yields."

[56] J. Mei, N. L. C. Leung, R. T. K. Kwok, J. W. Y. Lam, and B. Z. Tang, "Aggregation-Induced Emission," *Chemical Reviews*, 2015.

[57] P. Pander, P. Data, and F. B. Dias, "Time-resolved Photophysical Characterization of Triplet-harvesting Organic Compounds at an Oxygen-free Environment Using an iCCD Camera," *Journal of Visualized Experiments*, 2018.

[58] C. Ye, V. Gray, J. Mårtensson, and K. Bo, "Annihilation Versus Excimer Formation by the Triplet Pair in Triplet − Triplet Annihilation Photon Upconversion," 2019.

[59] Y. Y. Cheng, T. Khoury, M. J. Crossley, and T. W. Schmidt, "On the efficiency limit of triplet – triplet annihilation for photochemical upconversion," *Physical Chemistry Chemical Physics*, 2010.

[60] P. Pander, S. Gogoc, M. Colella, P. Data, and F. B. Dias, "Thermally Activated Delayed Fluorescence in Polymer-Small-Molecule Exciplex Blends for Solution-Processed Organic Light-Emitting Diodes," *ACS Applied Materials and Interfaces*, 2018.

[61] R. Komatsu, H. Sasabe, S. Inomata, Y. J. Pu, and J. Kido, "High efficiency solution processed OLEDs using a thermally activated delayed fluorescence emitter," *Elsevier*, 2015.

[62] L. Leonat, G. Sb, I. V. Br, and I. Cyclic, "Cyclic Voltammetry for energy levels estimation of organic materials," 2013.

[63] H.-B. Kim and J.-J. Kim, "Recent progress on exciplex-emitting OLEDs," *Journal of Information Display*, 2019.

[64] M. Chapran *et al.*, "Realizing 20% External Quantum Efficiency in Electroluminescence with Efficient Thermally Activated Delayed Fluorescence from an Exciplex," *ACS Applied Materials and Interfaces*, 2019.

[65] I. W. Wu, Y. H. Chen, P. S. Wang, C. G. Wang, S. H. Hsu, and C. I. Wu, "Correlation of energy band alignment and turn-on voltage in organic light emitting diodes," *Applied Physics Letters*, 2010.

[66] A. Udhiarto, L. M. Haryanto, B. Khoerun, and D. Hartanto, "Effect of anode and cathode workfunction on the operating voltage and luminance of a single emissive layer organic light emitting diode," *15th International Conference on Quality in Research (QiR): International Symposium on Electrical and Computer Engineering*, 2017.

[67] L. Qi, F. Just, G. Leuchs, and M. V. Chekhova, "Autonomous absolute calibration of an ICCD camera in single-photon detection regime," *Optics Express*, 2016.

[68] N. Elgrishi, K. J. Rountree, B. D. McCarthy, E. S. Rountree, T. T. Eisenhart, and J. L. Dempsey, "A Practical Beginner's Guide to Cyclic Voltammetry," *Journal of Chemical Education*, 2018.

Appendices

A. Materials properties and safety information

Table 1. Chloroform properties and safety information.

Chloroform For Spectroscopy Uvasol®	
Empirical formula	CHCl3
Molecular weight	119.38
Purity	≥ 99.0 %
Boiling point	61 °C
Symbol	
Hazard statements	H302, H315, H319, H331, H351, H361d, H372
Precautionary statements	P201 + P202 + P260 + P264 + P270 + P271 + P280
CAS number	67-66-3
Company	Sigma-Aldrich

Table 2. List of all used hosts and respective information.

	Polystyrene	**mCP**	**OXD-7**	**PO-T2T**
Chemical Formula	$(C_8H_8)_n$	$C_{30}H_{20}N_2$	$C_{30}H_{30}N_4O_2$	$C_{57}H_{42}N_3O_3P_3$
Molecular weight (g/mol)	104.10	408.49	478.58	909.80
Melting point	240 °C	176 °C	241 °C	221 °C
Maximum Absorption	260 nm (THF)	292 nm 338 nm (THF)	292 nm (THF)	272 nm (CH_2Cl_2)
Fluorescence emission	285 nm 332 nm (THF)	345 nm 360 nm (THF)	347 nm (THF)	295 nm 379 nm (CH_2Cl_2)
HOMO (eV)	7.5	6.1	6.5	6.8
LUMO (eV)	2.5	2.4	3.0	2.8
CAS Number	9003-53-6	550378-78-4	138372-67-5	1646906-26-4

B. Time-resolved gated luminescence setup

In the setup shown in Figure 20, the excitation is achieved with a nitrogen pulsed laser, NML 100, working at 10 Hz repetition rate with 3 ns pulse width. Using mirrors and a beam splitter, not represented on the schematic, the beam is directed to the sample holder. The resulting beam passes through convergent lenses to collimate and focus and is then collected through the spectrograph and detected by the iCCD camera, which is connected to the computer.

The luminescence decay is registered by changing the delay time and, in order to keep a good signal to noise ratio, also the integration time is adjusted over the measurement following a logarithmic law. The data obtained is corrected by dividing the integrated signal by the corresponding integration time, recording the emission decay. [57], [67]

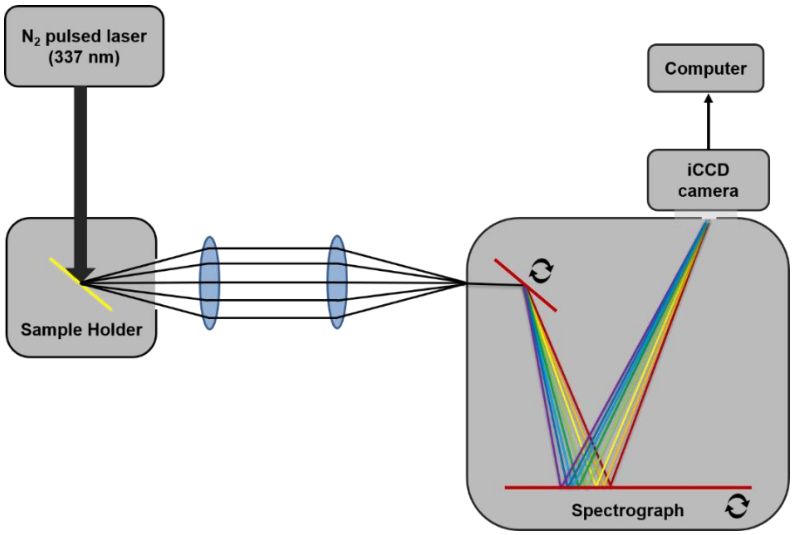

Figure 20. Time-resolved gated luminescence apparatus scheme.

C. Cyclic voltammetry procedure and apparatus

Starting with the measurement of the electrolyte solution to acquire the background signal and check possible contaminations, followed by the addition of ferrocene to determine the oxidation and reduction potentials of the standard, and then the measurement of the ARC-1476 compound in the electrolyte solution obtaining the voltammogram studied throughout this dissertation. In the end, a small amount of ferrocene is also added to the solution (ARC-1476 + electrolyte) to double-check the quality of the measurement. [62]

It is worth to note that to determine the reduction potential the solution was purged with argon gas to remove the oxygen, once its reduction potential is within the used potential scan range. [62], [68]

The schematic shown in Figure 21 resembles the electrode connections and the electrode positions during the measurements. Herein, a silver electrode was used as a reference while both working and counter were platinum electrodes.

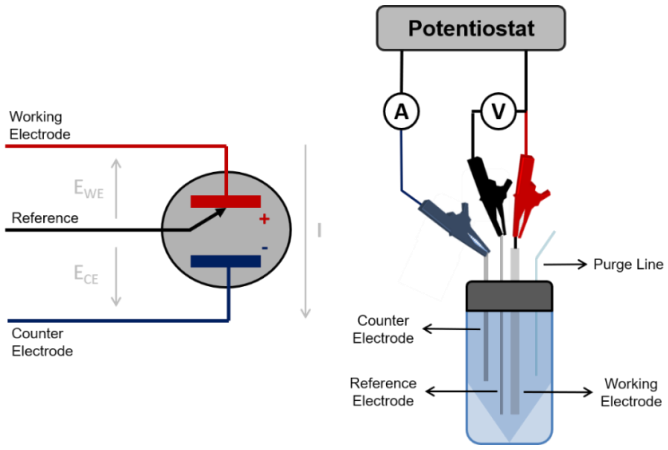

Figure 21. Electrode connections (left) and electrochemical cell (right) used on cyclic voltammetry.

D. Photoluminescence quantum yield spectra

Data obtained and used to determination of PLQY in solution.

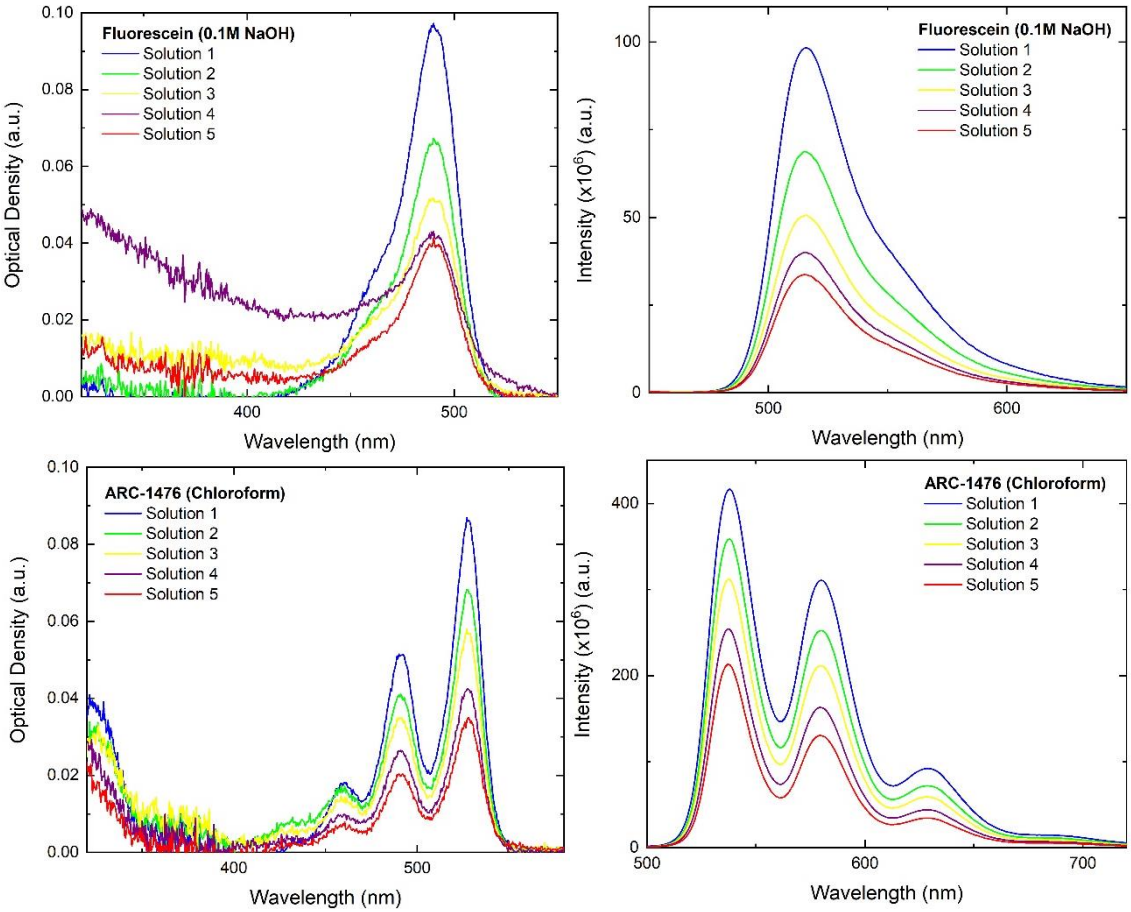

Figure 22. Data obtained for PLQY determination in solution. (a) Absorption spectra of five different solutions of fluorescein; (b) Emission spectra of the same five solutions obtained with an excitation wavelength of 490 nm; (c) Absorption spectra of five different solutions of ARC-1476; (d) Emission spectra of the same five solutions obtained with an excitation wavelength of 490 nm.

Data obtained and used to determination of PLQY in solid-state.

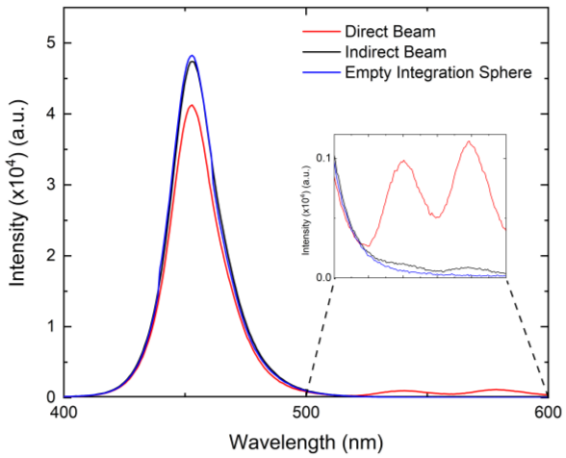

Figure 23. Fluorescence emission spectra obtained for the three measurements used for PLQY determination in solid-state. Direct excitation of the sample (red), indirect excitation (black) and empty integration sphere (blue).

E. Donor time-resolved fluorescence decay

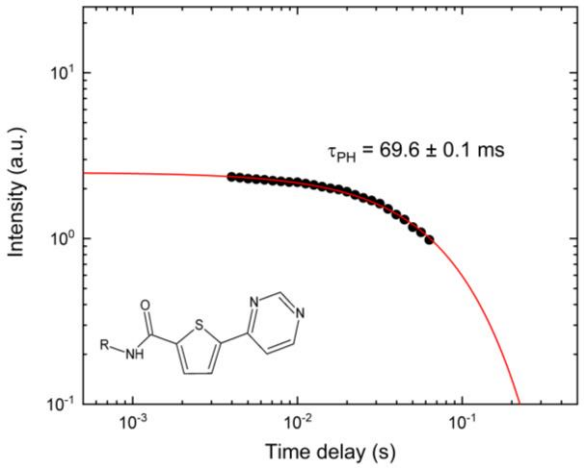

Figure 24. Time-resolved fluorescence decay curve of the donor. λ_{ex} = 355 nm.

F. Supplementary Steady-state information

The ARC-1476 emission and excitation spectrum were determined in a similar manner by monitoring the fluorescence emission and excitation scanning at various wavelengths. Excitation wavelengths were chosen by the peaks obtained from the absorption spectrum, while the emission wavelengths used for excitation spectra shown in Figure 25 (b) were based on the emission peaks of the compound.

The result of this study was used to check possible interference between an excitation source and the emission of the sample. When a significative overlap between the lower wavelength end of the emission spectrum and the higher wavelength end of the excitation spectrum occurs, this region must be eliminated using an excitation filter, to avoid the brighter excitation light overwhelms the weaker emitted fluorescence light.

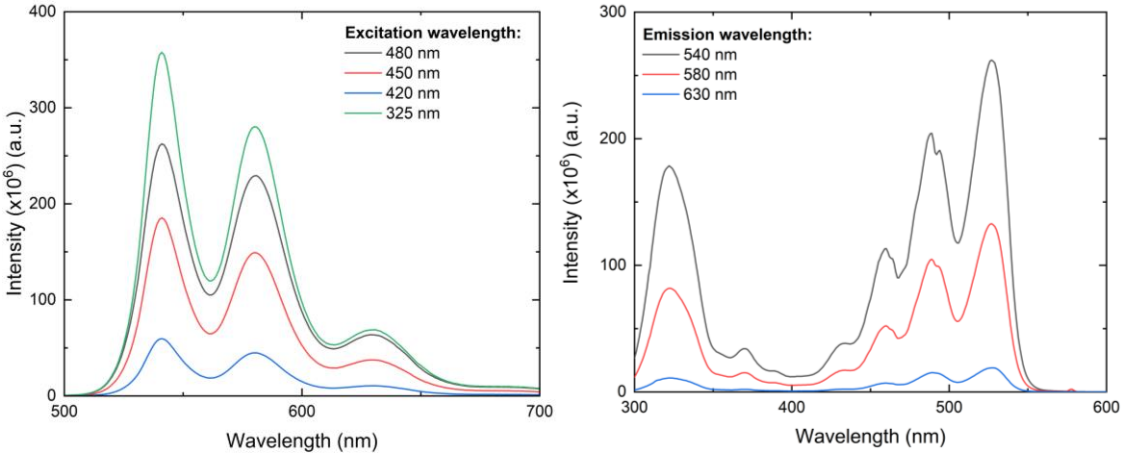

Figure 25. (a) The emission spectrum of ARC-1476 at different excitation wavelengths; (b) Excitation spectrum of ARC-1476 at different emission wavelengths.

G. Published poster

13th International Conference on Optical Probes of Organic and Hybrid Optoelectronic Materials and Applications, 7-12th July 2019, Vilnius, Lithuania

Triplet-to-Singlet Energy Transfer Mechanism

[1]Inês G. Tavares, [1]Piotr Pander, [2]Asko Uri, [2]Erki Enkvist, [1]Fernando B.Dias

Durham University

Centre for Materials Physics, OEM Group
[1]Department of Physics, Durham University, UK
[2]Institute of Chemistry, University of Tartu, Estonia

Introduction: Here we report the photophysical investigation of a novel compound showing triplet to singlet energy transfer between donor (D) and acceptor (A) units covalently linked. The energy transfer mechanism occurring upon excitation of the D unit involves initial ISC between the singlet and triplet states of the D unit, occurring in competition with singlet energy transfer between the singlet states of the D and A units, followed by barrierless triplet to singlet energy transfer from the D to A unit.

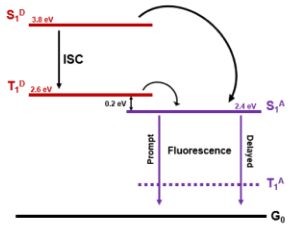

Figure 1. *Schematic of triplet energy transfer.*

Steady-state Spectroscopy

Compound and D unit

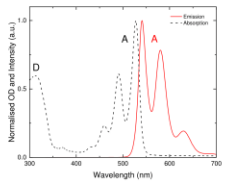

Figure 2. *Normalised absorption and emission spectra of the compound in solution.*

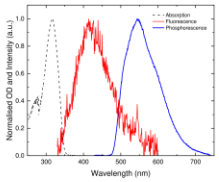

Figure 3. *Normalised absorption and emission spectra of the donor unit in solution. Phosphorescence spectrum was recorded in zeonex at 80 K.*

When the compound is excited with a 325 nm wavelength (donor absorption) the emission spectrum is composed by fluorescence of the acceptor only. Neither fluorescence or phosphorescence of the D is observed.

Time-resolved Spectroscopy

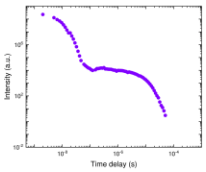

Figure 4. *Prompt and delayed fluorescence decay in solution. $\lambda_{excitation}$ = 337 nm.*

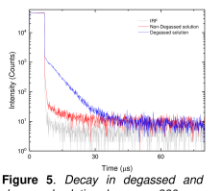

Figure 5. *Decay in degassed and non-degassed solution. $\lambda_{excitation}$ = 330 nm.*

The compound shows prompt and delayed fluorescence at room temperature.

Table 1. Prompt and delayed fluorescence lifetime.

	τ
Prompt Fluorescence	4.92 ns
Delayed Fluorescence	6.02 µs

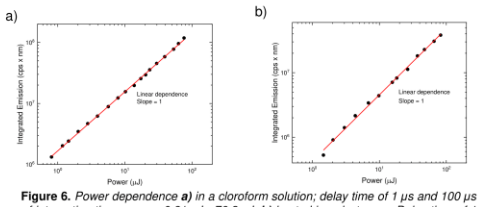

Figure 6. *Power dependence **a)** in a cloroform solution; delay time of 1 µs and 100 µs of integration time, power: 0.81 µJ - 76.2 µJ. **b)** hosted in polystyrene. Delay time of 1 µs and 20 µs of integration time, power: 1.46 µJ - 82.3 µJ.*

The compound shows a linear dependence (slope = 1) with the excitation dose both in solution and in solid state.

⇩

Intramolecular mechanism

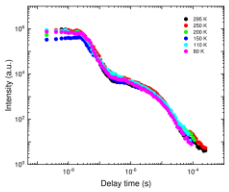

$T_1^D - S_1^A = 0.2$ eV

Due to barrierless triplet to singlet energy transfer from the donor to the acceptor, respectively, the luminescence decay is independent of the temperature.

Figure 7. *Decay as a function of temperature.*

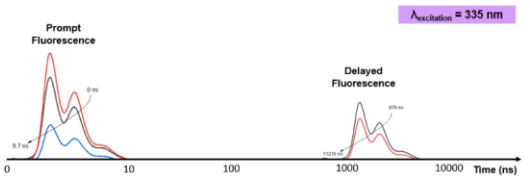

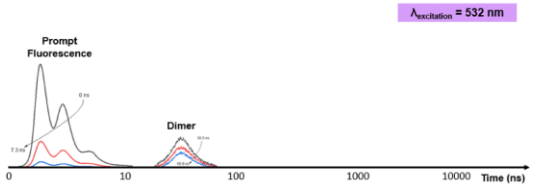

Figure 8. *Emission in a time scale (solid state).*

Is not observed delayed fluorescence when the compound is excited only on the acceptor.

Summary

In summary, a new way to promote triplet harvesting is reported. We explore triplet-to-singlet energy transfer between donor and acceptor units. The mechanism is in some ways analogous to TADF (Thermally Activated Delayed Fluorescence) but not involving charge transfer states, and thus allowing for observation of narrower emission spectra and larger flexibility in molecular design.